PI 1190701

THE UNITED STATES OF AMERICA

TO ALL TO WHOM THESE PRESENTS SHALL COME:

UNITED STATES DEPARTMENT OF COMMERCE
United States Patent and Trademark Office

July 12, 2004

THIS IS TO CERTIFY THAT ANNEXED HERETO IS A TRUE COPY FROM THE RECORDS OF THE UNITED STATES PATENT AND TRADEMARK OFFICE OF THOSE PAPERS OF THE BELOW IDENTIFIED PATENT APPLICATION THAT MET THE REQUIREMENTS TO BE GRANTED A FILING DATE.

APPLICATION NUMBER: *60/444,078*
FILING DATE: *January 31, 2003*
RELATED PCT APPLICATION NUMBER: *PCT/US04/02929*

By Authority of the
COMMISSIONER OF PATENTS AND TRADEMARKS

M. Tarver

M. TARVER
Certifying Officer

60/44078 .013103

01-03-03

A/PRV

Express Mail Label No. EL645096566US

01/31/03 1032 U.S. PTO

Please type a plus sign (+) inside this box → [+]

PTO/SB/16 (8-00)
Approved for use through10/31/2002.
U.S. Patent and Trademark Office; U.S. DEPARTMENT OF COMMERCE
Under the Paperwork Reduction Act of 1995, no persons are required to respond to a collection of information unless it displays a valid OMB control number.

01/31/03 1100 U.S. PTO 60/44078

PROVISIONAL APPLICATION FOR PATENT COVER SHEET

This is a request for filing a PROVISIONAL APPLICATION FOR PATENT under 37 CFR 1.53(c).

INVENTOR(S)		
Given Name (first and middle [if any])	Family Name or Surname	Residence (City and either State or Foreign Country)
Dong-Kyun	Seo	Phoenix, AZ

☑ *Additional inventors are being named on the* 1 *separately numbered sheets attached hereto*

TITLE OF THE INVENTION (280 characters max)

A NEW METHOD UTILIZING BORON SULFIDES AND SELENIDES FOR THE SYNTHESES OF. . . .

Direct all correspondence to: **CORRESPONDENCE ADDRESS**

☑ Customer Number 26707 →

OR *Type Customer Number here*

26707
PATENT TRADEMARK OFFICE

☐ Firm or Individual Name					
Address					
Address					
City		State		ZIP	
Country		Telephone		Fax	

ENCLOSED APPLICATION PARTS *(check all that apply)*

☑ Specification *Number of Pages* 33
☐ Drawing(s) *Number of Sheets*
☐ Application Data Sheet. See 37 CFR 1.76
☐ CD(s), Number
☑ Other (specify) Return Postcard

METHOD OF PAYMENT OF FILING FEES FOR THIS PROVISIONAL APPLICATION FOR PATENT

☑ Applicant claims small entity status. See 37 CFR 1.27.
☐ A check or money order is enclosed to cover the filing fees
☑ The Commissioner is hereby authorized to charge filing fees or credit any overpayment to Deposit Account Number: 17-0055
☐ Payment by credit card. Form PTO-2038 is attached.

FILING FEE AMOUNT ($): 80.00

The invention was made by an agency of the United States Government or under a contract with an agency of the United States Government.

☑ No.
☐ Yes, the name of the U.S. Government agency and the Government contract number are: _____

Respectfully submitted,

SIGNATURE Christine M. Meis

Date 1 / 31 / 03

TYPED or PRINTED NAME Christine M. Meis

REGISTRATION NO. *(if appropriate)* 52,024

Docket Number: 130588.00002

TELEPHONE (602) 229-5247

USE ONLY FOR FILING A PROVISIONAL APPLICATION FOR PATENT

This collection of information is required by 37 CFR 1.51. The information is used by the public to file (and by the PTO to process) a provisional application. Confidentiality is governed by 35 U.S.C. 122 and 37 CFR 1.14. This collection is estimated to take 8 hours to complete, including gathering, preparing, and submitting the complete provisional application to the PTO. Time will vary depending upon the individual case. Any comments on the amount of time you require to complete this form and/or suggestions for reducing this burden, should be sent to the Chief Information Officer, U.S. Patent and Trademark Office, U.S. Department of Commerce, Washington, D.C. 20231. DO NOT SEND FEES OR COMPLETED FORMS TO THIS ADDRESS. SEND TO: Box Provisional Application, Assistant Commissioner for Patents, Washington, D.C. 20231.

1713776

Express Mail Label No. EL645096566US

PROVISIONAL APPLICATION COVER SHEET
Additional Page

PTO/SB/16 (8-00)
Approved for use through 10/31/2002.
U.S. Patent and Trademark Office; U.S. DEPARTMENT OF COMMERCE

Under the Paperwork Reduction Act of 1995, no persons are required to respond to a collection of information unless it displays a valid OMB control number.

Docket Number	130588.00002	Type a plus sign (+) inside this box →	+

INVENTOR(S)/APPLICANT(S)		
Given Name (first and middle [if any])	Family or Surname	Residence (City and either State or Foreign Country)
Li-Ming	Wu	Tempe, AZ

Number 1 of 1

WARNING: Information on this form may become public. Credit card information should not be included on this form. Provide credit card information and authorization on PTO-2038.

Express Mail Label No. EL645096566US

PTO/SB/17 (1-03)
Approved for use through 10/31/2003.
U.S. Patent and Trademark Office; U.S. DEPARTMENT OF COMMERCE
Under the Paperwork Reduction Act of 1995, no persons are required to respond to a collection of information unless it displays a valid OMB control number.

FEE TRANSMITTAL for FY 2003

Patent fees are subject to annual revision.

☑ Applicant claims small entity status. See 37 CFR 1.27

TOTAL AMOUNT OF PAYMENT ($) 80.00

Complete if Known	
Application Number	
Filing Date	Filed concurrently herewith
First Named Inventor	Dong-Kyun Seo
Examiner Name	
Group Art Unit	
Attorney Docket No.	130588.00002

METHOD OF PAYMENT *(check all that apply)*

☐ Check ☐ Credit card ☐ Money Order ☐ Other ☐ None

☑ Deposit Account:

Deposit Account Number: 17-0055

Deposit Account Name: Quarles & Brady LLP

The Commissioner is authorized to: *(check all that apply)*

☑ Charge fee(s) indicated below ☑ Credit any overpayments

☑ Charge any additional fee(s) during the pendency of this application

☐ Charge fee(s) indicated below, except for the filing fee to the above-identified deposit account.

FEE CALCULATION

1. BASIC FILING FEE

Large Entity Fee Code	Large Entity Fee ($)	Small Entity Fee Code	Small Entity Fee ($)	Fee Description	Fee Paid
1001	750	2001	375	Utility filing fee	
1002	330	2002	165	Design filing fee	
1003	520	2003	260	Plant filing fee	
1004	750	2004	375	Reissue filing fee	
1005	160	2005	80	Provisional filing fee	80.00

SUBTOTAL (1) ($) 80.00

2. EXTRA CLAIM FEES FOR UTILITY AND REISSUE

		Extra Claims		Fee from below	Fee Paid
Total Claims	-20** =		X		=0.00
Independent Claims	-3** =		X		=0.00
Multiple Dependent					=

Large Entity Fee Code	Large Entity Fee ($)	Small Entity Fee Code	Small Entity Fee ($)	Fee Description
1202	18	2202	9	Claims in excess of 20
1201	84	2201	42	Independent claims in excess of 3
1203	280	2203	140	Multiple dependent claim, if not paid
1204	84	2204	42	** Reissue independent claims over original patent
1205	18	2205	9	** Reissue claims in excess of 20 and over original patent

SUBTOTAL (2) ($) 0.00

**or number previously paid, if greater; For Reissues, see above

FEE CALCULATION (continued)

3. ADDITIONAL FEES

Large Entity Fee Code	Large Entity Fee ($)	Small Entity Fee Code	Small Entity Fee ($)	Fee Description	Fee Paid
1051	130	2050	65	Surcharge - late filing fee or oath	
1052	50	2052	25	Surcharge - late provisional filing fee or cover sheet	
1053	130	1053	130	Non-English specification	
1812	2,520	1812	2,520	For filing a request for *ex parte* reexamination	
1804	920*	1804	920*	Requesting publication of SIR prior to Examiner action	
1805	1,840*	1805	1,840*	Requesting publication of SIR after Examiner action	
1251	110	2251	55	Extension for reply within first month	
1252	410	2252	205	Extension for reply within second month	
1253	930	2253	465	Extension for reply within third month	
1254	1,450	2254	725	Extension for reply within fourth month	
1255	1,970	2255	985	Extension for reply within fifth month	
1401	320	2401	160	Notice of Appeal	
1402	320	2402	160	Filing a brief in support of an appeal	
1403	280	2403	140	Request for oral hearing	
1451	1,510	1451	1,510	Petition to institute a public use proceeding	
1452	110	2452	55	Petition to revive - unavoidable	
1453	1,300	2453	650	Petition to revive - unintentional	
1501	1,300	2501	650	Utility issue fee (or reissue)	
1502	470	2502	235	Design issue fee	
1503	630	2503	315	Plant issue fee	
1460	130	1460	130	Petitions to the Commissioner	
1807	50	1807	50	Processing fee under 37 CFR 1.17(q)	
1806	180	1806	180	Submission of Information Disclosure Stmt	
8021	40	8021	40	Recording each patent assignment per property (times number of properties)	
1809	750	2809	375	Filing a submission after final rejection (37 CFR § 1.129(a))	
1810	750	2810	375	For each additional invention to be examined (37 CFR § 1.129(b))	
1801	750	2801	375	Request for Continued Examination (RCE)	
1802	900	1802	900	Request for expedited examination of a design application	

Other fee (specify) _____

*Reduced by Basic Filing Fee Paid SUBTOTAL (3) ($) 0.00

SUBMITTED BY				Complete *(if applicable)*	
Name (Print/Type)	Christine M. Meis	Registration No. (Attorney/Agent)	52,024	Telephone	(602) 229-5247
Signature	Christine M. Meis			Date	1/31/03

WARNING: Information on this form may become public. Credit card information should not be included on this form. Provide credit card information and authorization on PTO-2038.

1713777

Burden Hour Statement: This form is estimated to take 0.2 hours to complete. Time will vary depending upon the needs of the individual case. Any comments on the amount of time you are required to complete this form should be sent to the Chief Information Officer, U.S. Patent and Trademark Office, Washington, DC 20231. DO NOT SEND FEES OR COMPLETED FORMS TO THIS ADDRESS. SEND TO: Commissioner for Patents, Washington, DC 20231.

EXPRESS MAIL CERTIFICATE: EL645096566US

I hereby certify that this correspondence listed below is being deposited with the United States Postal Service on the date set forth below as Express Mail in an envelope addressed to: BOX Provisional Patent Application, Commissioner for Patents, Washington, D.C. 20231

Date of Signature and Deposit: 1-31-03

By Teri Weissert
(Signature of person depositing mail)
Teri Weissert

CERTIFICATE OF MAILING PURSUANT TO 37 C.F.R. 1.10

Applicant: Dong-Kyun Seo
Filed: Concurrently herewith
Title: A New Method Utilizing Boron Sulfides And Selenides For The Syntheses Of Nanostructured Metal Sulfides And Selenides From Metals And Metal Oxides
Docket No.: 130588.00002

BOX Provisional Patent Application
Commissioner for Patents
Washington, D.C. 20231

Type of Filing:

1) Fee Transmittal
2) Provisional Application For Patent Cover Sheet
3) Patent Application (33 pages)
4) Return receipt postcard

APPLICATION

BY

DONG-KYUN SEO

AND

LI-MING WU

FOR

UNITED STATES PATENT

ON

A NEW METHOD UTILIZING BORON SULFIDES AND SELENIDES FOR THE SYNTHESES OF NANOSTRUCTURED METAL SULFIDES AND SELENIDES FROM METALS AND METAL OXIDES

Docket No.: 130588.00002
Express Mail Label No.: EL645096566US

Pages of Application: 33
Sheets of Drawings: 0

BRIEF SUMMARY OF THE INVENTION:

Utilization of boron sulfides and selenides have not reported before for preparation of inorganic metal sulfides and selenides. We found that they could be versatile sources of sulfur and selenium in converting many different metals including transition and rare-earth metals and their oxides. The reaction scheme is very simple and easily transferable to industrial scale synthesis. Intermediate or low temperature reaction condition allows various nanostructures of sulfides and selenides. The metal sulfides and selendies are used in lubrication, catalysis, battery applications and so on. The new method can provide new nanostructured chalcogenide materials via very simple processes which have not forseen before.

DETAILED DESCRIPTION OF THE INVENTION:

We found that boron sulfides could be a versatile source of sulfur in oxidative sulfidation of metals as well as in sulfidation of various metal oxides at low temperatures. Our experimental results indicate that the sulfidation can be carried out in the temperature region of 300–600°C, without any visible damages of silica containers. The low-temperature operation could have an advantage in preparing nanostructured materials, because the competing crystal-growth processes can be suppressed due to the low thermal energy. Furthermore, it allows us to access the compounds that exist only at low temperatures and decompose at elevated temperatures. The boron sulfides can be prepared *in situ* in an evacuated and sealed silica tube which is loaded with boron, sulfur and the material that is to be sulfidized. The materials to be sulfidized can be elemental metals, or binary/ternary transition-metal oxides. The reactions occur at the solid-gas boundaries, and yet are carried out in a sealed container, which eliminates the need of continuous flow of sulfidizing gases such as H_2S and CS_2. Neither does the container need to be pressurized as in the synthetic routes that utilize elemental sulfur. These allow us to afford a much simpler experimental setup that is inherently safe from possible explosions or leakage of harmful gases. The boron sulfides left after the sulfidation can be recycled by sublimation, which is particularly desirable for large-scale industrial production. Otherwise, they readily react with water or alcohols to form H_2S and boron hydroxide, and can be washed away from the products.

We also found boron selenides can be effective selenidizing agents, and the experimental produres for selenization is very much close to the sulfurization produres with boron sulfides.

We believe the method is genetic, which our recent experimental results demonstrate as the following:

(1) Preparation of *ultralong* TaS_3 nanowires from Ta metal. The reactions of Ta thin metal pieces with B_2S_3 at 400-500 °C resulted in bundles of nanowires of TaS_3 that grew from the surface of the metal pieces. The wires were 10-200 nm wide along the transverse direction, and their length varies from several microns, to millimeters, even to several centimeters, depending on the synthetic conditions. Bundles of wires longer than 2 cm are quite common, and we once observed hairy bundles (< 0.01 mm wide) that were longer than 5 cm. We obtained similar results for $TaSe_3$ and $NbSe_3$. The fibrous structure provides particularly

desirable characteristics for battery applications because of the high surface area. The test results in 1970s on the batteries with these fibrous trisulfides as a positive electrode showed that those batteries maintained a large fraction of their capacity after being recharged a large number of times, and yielded attractive capacities.

(2) **Preparation of WS_2 and MoS_2 nanoparticles via direct sulfurization of tungsten metal at low temperatures.** With boron sulfides, we could sulfidize tungsten and molybdenum metal wires (0.2 mm in diameter, ~5 cm long) completely into WS_2 at 600 °C in 24 hours. The product maintained the original shape of the tungsten wires, and yet with a roughly doubled thickness. Sublimation of the remaining boron sulfides and sulfur and/or washing in water provided the disulfide nanomaterials with a purity higher than 99.9%. WS_2 and MoS_2, which show numerous desirable properties in the fields of catalysis, electrocatalysis, electrochemical intercalation and lubrication. For efficient applications of their chemical properties, the WS_2, and MoS_2, materials need to be prepared with high surface areas, and hence their nanostructures are highly desirable.

(3) **Preparation of TiS_2 nanoparticles and nanorods from TiO_2 nanoparticles.** Nanoparticles of TiO_2 were converted to TiS_2 or TiS_3 nanoparticles in the temperature region between 300 and 450 °C depending on the loaded ration of boron and sulfur as well as the reaction temperatures. In TEM images of the sample from the reactions, nanoparticles (< 40 nm) and nanorods (~120 nm wide and > 3 um long) were found. The layered structure of TiS_2 makes the compound suitable for use as high-temperature lubricants, and electrode materials for high-density lithium batteries.

(4) **Preparation of FeS_2 nanoparticles from $FeSiO_3$ micoparticles.** $FeSiO_3$ became completely decomposed into binary sulfides, FeS_2 and SiS_2, during the sulfidation process (destructive sulfidation). Interestingly, the starting material was microcrystalline, but the product seemed to be nanostructured. For example, the volume of the reaction mixture increased by about six times, and the product was a much finer and floppy powder. SiS_2 is reactive to water, and we could remove it along with boron sulfides by washing the product in deionized water. The X-ray powder pattern shows a pure phase of FeS_2. The preliminary SEM studies on the sample indicated that the size of the product powder was smaller than the resolution limit of our instrument, and TEM studies are under way. FeS_2 is a well-known battery material, and exhibits interesting quantum confinement effect when the size is smaller than 10 nm.

(5) **Preparation of NdS_2 nanoparticles from Nd_2O3 nanoparticles.** Nd_2O3 nanoparticles were completely sulfidized into NdS_2 nanoparticels at 450 °C in a day, and the color of the powder turned into grayish yellow from pale violet. We recognize that the product is not Nd_2S_3, the corresponding sulfide of Nd_2O_3, and this can be attributed to an incomplete reaction between boron and sulfur. The product was examined under a TEM microscope after dispersed in deionized water, and was found to generally maintain the original sizes after the sulfidation, as found in the TEM image. The particles appear to have a shape of thin disks. To our knowledge, the only rare-earth sulfide nanostructure reported in the literature to date is EuS nanoparticles that show an interesting luminescent characteristic. We believe our method is a general method for conversion of rare-earth metal oxides into their sulfides.

(6) Preparation of $BaTiS_3$ from $BaTiO_3$. $BaTiO_3$ microparticles could be converted into $BaTiS_3$ in a high yield at 450 °C with no visible fusion of the particles. The detailed analysis of the product is in progress, and the reactions will also be carried out for nanoparticles of $BaTiO_3$. It is noted that in the literature there have been no reports on nanostructured *ternary* transition-metal sulfides, to our knowledge.

It is noted that our experiments have been done by employing a typical solid-state synthetic scheme. We already commented in our recent NSF proposal that synthetic routes could be solvent reflux, solvothermal or sonochemical, by taking advantage of the chemical characteristics of boron chalcolgenides formed in solid at ambient condition, and we are currently investigating such possibilities.

List companies you believe might be interested in using, developing or marketing this invention.

[redacted]

PROJECT DESCRIPTION

Part I. Research Plan

I. Background and Motivation

Metal sulfides find applications as hydrotreating catalysts, as lubricants, as battery electrode materials, and in semiconductor, photocatalytic, and electrocatalytic devices.[1] While binary and ternary transition metal oxides are easily available in various nano-sized forms, however, the corresponding nanostructured sulfides are relatively rare despite their technological importance. Well-known examples of nanostructured chalcogenide materials include nanoparticles and nanotubes of WS_2 and MoS_2,[2] and their syntheses have been carried out by several different methods: the annealing of oxidized transition metal films or particles in a stream of H_2S gas;[2] template deposition using porous alumina;[3] electron beam irradiation in TEM[4a] and local heating via electrical pulse in STM[4b]; sonoelectrochemical bath reactions;[5] electrochemical deposition from an ethylene glycol solution;[6] inverse micelle synthesis;[7] and solution reaction of molybdenum hexacarbonyl with elemental sulfur.[8] Nanotubes of TaS_2 and NbS_2 have been synthesized recently by the reduction of TaS_3 and NbS_3 powders in a stream of H_2 at 1000 °C.[9] In addition, multiwalled carbon nanotubes have been used as a template to produce NbS_2, WS_2 and ReS_2 nanotubes.[10] FeS_2 particles with < 10 nm have been synthesized via inverse micelle technique.[11] Solvothermal methods also have been applied for the preparation of nanocrystalline transition-metal sulfides by employing elemental sulfur as a sulfidizing agent in organic media.[12] To our knowledge, however, no nanostructured *ternary* transition-metal chalcogenides have been reported in the literature.

We recently found that boron sulfides could be a versatile source of sulfur in oxidative sulfidation of metals as well as in sulfidation of various metal oxides at low temperatures. To date, boron sulfides (B_2S_3 and BS_2) have not been familiar sulfidizing agents, and their use has been reported only in organic or organometallic reactions, yet sporadically.[13] The main body of the solid state reactions involving boron sulfides have been limited to the synthesis of crystalline or amorphous thioborates with the early main-group metals, silver, lead or thalium.[14] There exist only two boron sulfides, B_2S_3 and BS_2, in the sulfur-rich end, and both of the air-sensitive compounds are normally obtained in amorphous state.[15] B_2S_3 does not have a well-defined melting point, but begins to sublime at about 300 °C.[16] BS_2, the only boron sulfide with a higher content of sulfur, melts congruently at 417 °C under atmospheric pressure. However, our experiences show that a significant amount of BS_2 evaporates even at 300 °C under vacuum. The extremely corrosive nature of the boron sulfide compounds is probably the main reason for their scarce use in solid state reactions, and indeed the silica reaction vessels need to be heavily carbon-coated for the synthesis of the alkali thioborates which is carried out typically above 600 °C.[14] Another reason can be found in the fact that there do not exist any transition-metal thioborates other than silver compounds.[14, 17] The original report[18] on the existence of MnB_2S_4 was a misidentification of Mn_2SiS_4 that was formed by the undesirable reaction of boron sulfides with unprotected silica containers under a high-temperature reaction condition.[19] In this respect, the chemical properties of boron sulfides are in contrast to those of phosphorous sulfides which often form ternary or quaternary compounds with active metals and/or transition metals.[20]

While boron sulfides are not much promising in discovery of new compounds that incorporate boron, it is evident that the extremely corrosive nature of boron sulfides might

provide a great opportunity as sulfidizing agents that operate at lower temperatures. Indeed, our preliminary experimental results indicate that the sulfidation can be carried out in the temperature region of 300 – 600 °C, without any visible damages of silica containers. The low-temperature operation could have an advantage in preparing nanostructured materials, because the competing crystal-growth processes can be suppressed due to the low thermal energy. Furthermore, it allows us to access the compounds that exist only at low temperatures and decompose at elevated temperatures. The boron sulfides can be prepared *in situ* in an evacuated and sealed silica tube which is loaded with boron, sulfur and the material that is to be sulfidized. The materials to be sulfidized can be elemental metals, or binary/ternary transition-metal oxides. The reactions occur at the solid-gas boundaries, and yet are carried out in a sealed container, which eliminates the need of continuous flow of sulfidizing gases such as H_2S and CS_2. Neither does the container need to be pressurized as in the synthetic routes that utilize elemental sulfur. These allow us to afford a much simpler experimental setup that is inherently safe from possible explosions or leakage of harmful gases. The boron sulfides left after the sulfidation can be recycled by sublimation, which is particularly desirable for large-scale industrial production. Otherwise, they readily react with water or alcohols to form H_2S and boron hydroxide, and can be washed away from the products.

In the following, we show our recent preliminary results in developing new low-temperature synthetic methodologies for nanostructured transition-metal sulfides, and describe our research plans in extending our preliminary work during the proposed funding period.

II. Preliminary experimental results

(1) Preparation of *ultralong* TaS_3 nanowires from Ta metal.

The bulk TaS_3 is a well-known quasi-one-dimensional (quasi-1D) metal with a layered structure,[21] and it undergoes two charge density wave (CDW) transitions below room temperature.[22] It has been known that thin fibers of TaS_3, $TaSe_3$ and $NbSe_3$ can be obtained from the reactions between the transition-metal powders or thin films and elemental sulfur or selenium at the temperatures over 500 °C for sulfides and over 650 °C for selenides.[23] The fibrous structure provides particularly desirable characteristics for battery applications because of the high surface area.[24] The test results on the batteries with these fibrous trisulfides as a positive electrode showed that those batteries maintained a large fraction of their capacity after being recharged a large number of times, and yielded attractive capacities.[25] The highly 1D structure also gives rise to negative absolute resistance in the CDW sliding regime, which was confirmed from the electrical property measurements on the (sub)micron-scale fibers of TaS_3 and $NbSe_3$.[26] Most recently, a Japanese group reported ~1 μm wide Möbius strips of those trichalcogenides which were prepared with elemental sulfur or selenium over 740 °C.[27] However, nanowires of these compounds have not been reported up to now.

By utilizing boron sulfides as a sulfidizing agent in the lower temperature region, we could prepare nanowires of TaS_3 that were extremely long. The reactions of Ta thin metal pieces with B_2S_3 at 400 – 500 °C resulted in bundles of nanowires of TaS_3 that grew from the surface of the metal pieces. The wires were 10 – 200 nm wide along the transverse direction, and their length varies from several microns, to millimeters, even to several centimeters, depending on the synthetic conditions. Bundles of wires longer than 2 cm are quite common, and we once observed hairy bundles (< 0.01 mm wide) that were longer than 5 cm. For those wires, the

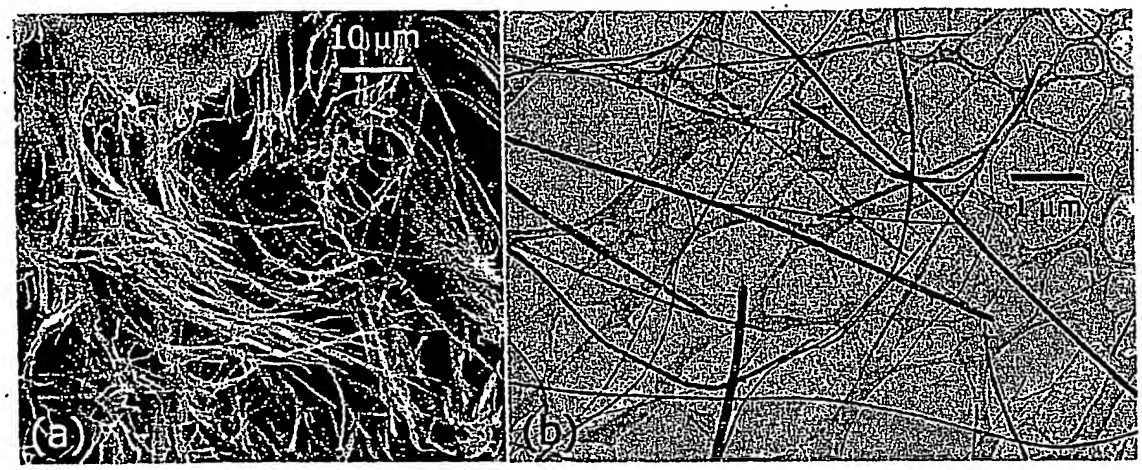

Figure 1. (a) SEM image of TaS_3 hairy wires and their bundles. The wires grow from the surfaces of the Ta metal pieces in the reaction container, and are free-standing. (b) TEM image of TaS_3 nanowires hanging on top of amorphous carbon grids (light gray).

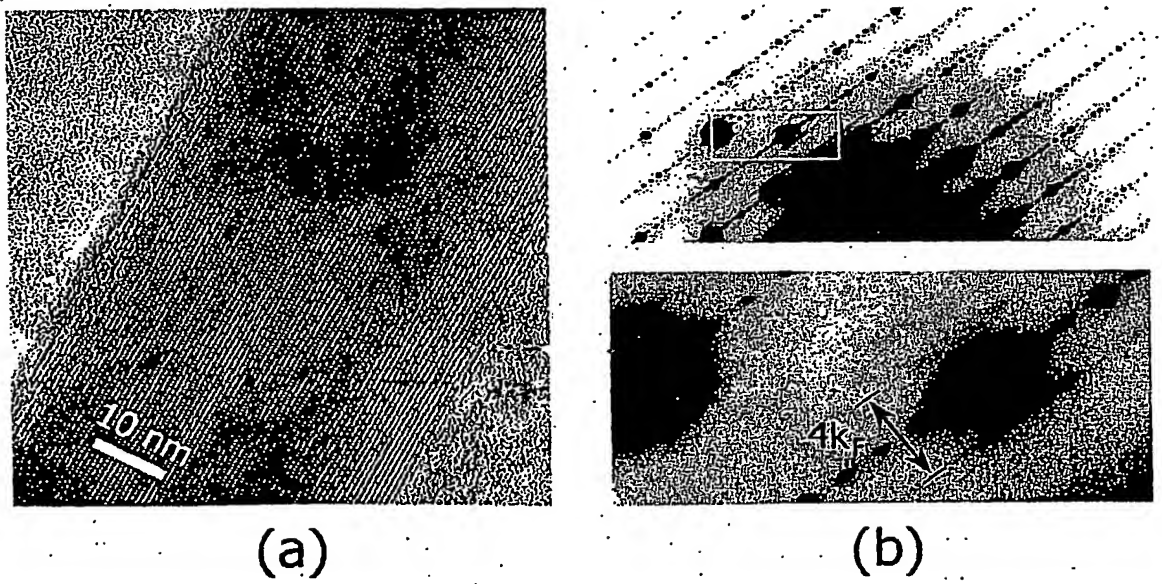

Figure 2. (a) TEM image of a TaS_3 nanowire. (b) Electron diffraction pattern of the wire in (a). The boxed area in the upper picture is magnified in the lower. Diffuse scattering is clearly seen. $4k_F$ (= $c^*/2$) corresponds to $2q$, where q is the CDW nesting vector.

aspect ratios could reach up to ~10^6! The long wires were fragile, and great care was necessary to handle them.

Figure 1 shows the SEM and TEM images of the wires grown from a Ta piece after one week of reaction. Although not shown here, the X-ray powder diffraction patterns of the products indicated that the products were pure without any other sulfides. The powder patterns were most similar to those of the orthorhombic structure of bulk TaS_3, rather than the monoclinic one. The two different structures are due to two different layer-stacking patterns, and further studies are necessary to elucidate precisely the stacking patterns in our nanowires. **Figure 2a** presents a TEM image of an individual ~50 nm-wide TaS_3 nanowire, and **Figure 2b** is the corresponding electron diffraction photograph taken at room temperature for the same nanowire. The well-defined diffraction spots indicate a good crystallinity. The calculated lattice parameters in the reciprocal plane were in a good agreement with the unit cell parameters of the TaS_3 layers in the bulk material.[28] The growth direction of the wires corresponds to the 1D chain direction of the bulk. The diffuse lines in **Figure 2b** are characteristic of the diffuse scatting caused by the disordered CDW modulations along the chain direction, and their locations and spacing match with the previous data.[29] The detailed structures of our TaS_3 nanowires need to be thoroughly examined, and our preliminary high-resolution TEM (HRTEM) work indicates ribbon-like nature of the wires.

(2) Preparation of WS_2 particles via direct sulfurization of tungsten metal at low temperatures.

The successful preparation of TaS_3 nanowires prompted us to try our new low-temperature synthetic method for other transition metals. Direct sulfidation of transition metals is usually carried out by using H_2S, and our anticipation is that the employment of boron sulfides may provide alternative or even better ways of tailoring the morphological and chemical properties of the sulfidized products. Exploration and development of new synthetic routes can be important particularly for sulfide catalysts, because sulfidation reactions are a crucial step in the preparation of the catalysts, and have a profound influence on the (surface) structure and on the dispersion of the catalytically active particles.[30] Another application of the new low-temperature sulfidation reactions is to convert metal nanoparticles into the corresponding metal sulfides while keeping their small sizes by avoiding significant fusion of the nanoparticles. This capability could become important in the future, as more and more metal nanoparticles become available owing to the advances in the development of synthetic techniques for metal nanoparticles.

Our preliminary experiments in this project have focused on the layered compounds, WS_2 and MoS_2, which show numerous desirable properties in the fields of catalysis, electrocatalysis, electrochemical intercalation and lubrication.[1, 31] For efficient applications of their chemical properties, the WS_2 and MoS_2 materials need to be prepared with high surface areas, and hence their nanostructures are highly desirable. Depending on their sizes, furthermore, nanoparticles of the disulfides show unique properties not present in bulk. For example, highly nanostructured MoS_2 made by sonochemical synthesis catalyzes thiophene hydrodesulfurization with higher activities than those of the otherwise most active (yet expensive) materials such as RuS_2 and $RuSe_2$.[5a]

Typical sulfidation of tungsten metal is carried out by H_2S at high temperatures. For example, WS_2 nanotubes and fullerene-like nanoparticles were first observed when very thin films of tungsten were sulfidated above 900 °C.[2a] With boron sulfides, however, we could sulfidize tungsten metal wires (0.2 mm in diameter, ~5 cm long) completely into WS_2 at 600 °C in 24 hours. The product maintained the original shape of the tungsten wires, and yet with a roughly doubled thickness. The surface exhibited severe cracks along the wire axis, and the product was easy to grind into a fine powder. As shown in **Figure 3**, the Bragg peaks are very broad in the X-ray power diffraction pattern, indicating small sizes of the powder particles. One intriguing feature is that the (00*l*) peaks are shifted toward lower angles, indicating the expansion of the lattice along the *c*-axis, in comparison with the bulk 2H-phase (vertical lines).[32] The shift of $\Delta c = 0.14$ Å was calculated using synthetic silicon as an internal standard for the powder diffraction studies. The same observation was made from our molybdenum sulfidation reactions. A similar shift has been reported for the fullerene-like and nanotubular structures of WS_2 and MoS_2 ($\Delta c = 0.16$ and 0.25 Å, respectively),[2b, 33] and attributed to a strain relief in the folded structures by expanding the spacing between adjacent layers. This has been known for carbon fullerenes and nanotubes as well.[34]

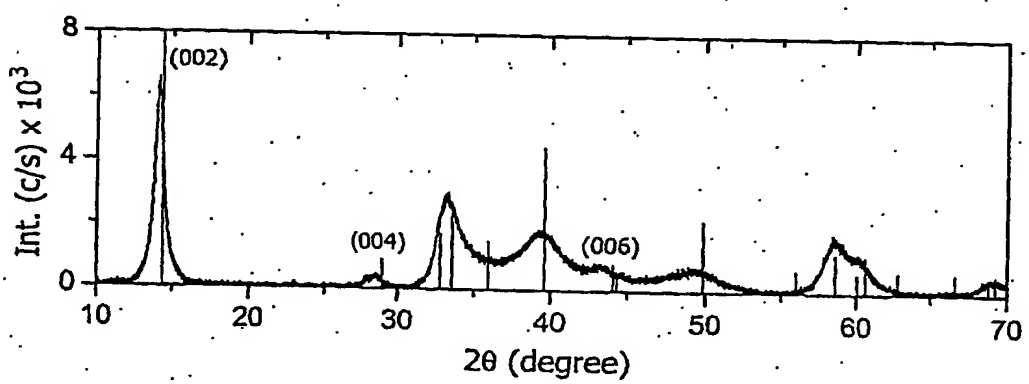

Figure 3. XRD powder pattern of the reaction product from the sulfidation of tungsten wire by boron sulfides. The vertical lines are the Bragg peaks of NBS 2H-WS_2. Note the shift of (00*l*) peaks. The (008) peak is very weak and cannot be seen due to the overlap with a peak of high intensity.

Figure 4a is an SEM image of the WS_2 powder material, in which the layered morphology of the compound can be clearly seen. The surfaces of the layers are severely cracked and highly corrugated, implying the high surface area of the powder product. The detailed structures of the product were studied with TEM, after the powder was ultrasonicated in deionized water. The dark fringes in the TEM images of **Figure 4b** and **4c** are spaced ~ 6.2 Å apart, which indicates that the fringes are the WS_2 layers oriented more or less parallel to the electron beam direction (the interlayer distance from the powder pattern = 12.54/2 Å = 6.27 Å). The fringes (layers) are highly fragmented, and the typical lengths of the fringe filaments range from 5 to 15 nm. The transverse dimensions across the fringes (i.e., along the layer-stacking direction) are even smaller, in general. The shapes of the nanostructures are highly irregular, but none of them can be considered to be fullerene-like or nanotubular because the fringes (layers)

do not merge at their ends. It is noted that the layer filaments are not always straight, but curled in general, especially near their ends. This significant deformation of the WS_2 layers occasionally causes the adjacent layers to come off from each other, as indicated by a big arrow in Figure 4c. The small arrow points a disconnection of an individual layer. Figure 4d presents a typical TEM image of the WS_2 layer planes (the layer planes perpendicular to the electron

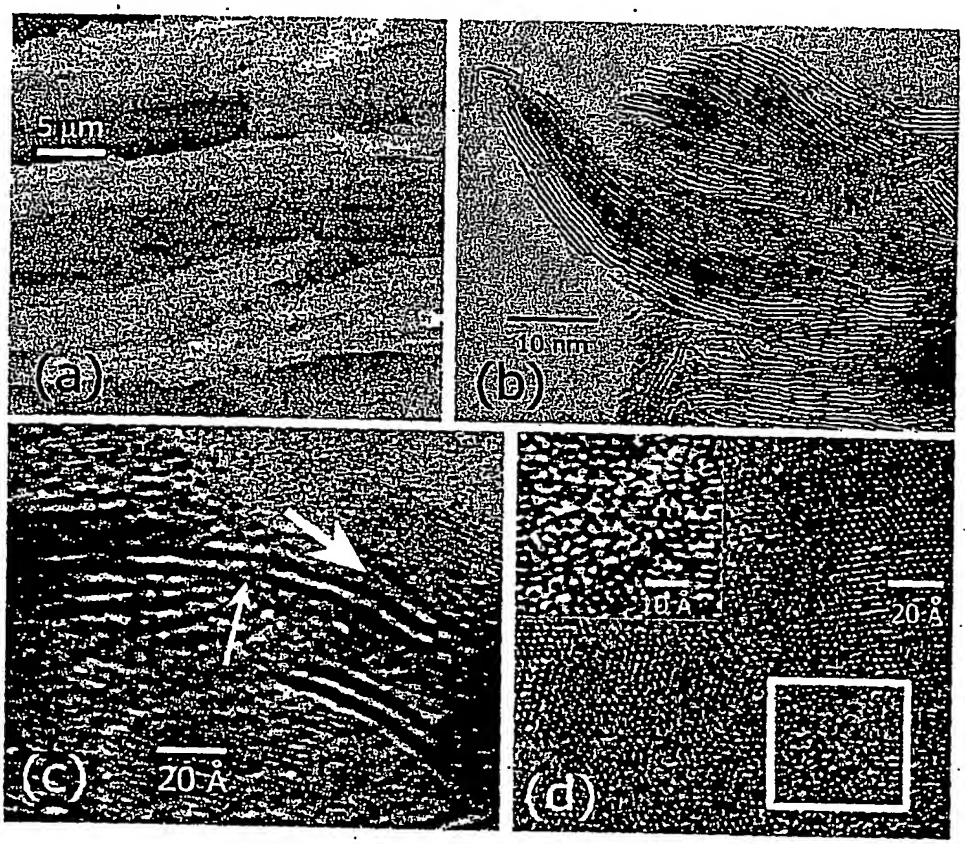

Figure 4. (a) SEM image of WS_2 pieces as prepared. (b) TEM image showing interwoven WS_2 layers. The dark fringes correspond WS_2 layers, and the fringe filaments look highly distorted and curved. (c) The big arrow indicates two layers coming off from each other, while the small arrow points a dislocation or crack in an individual layer. (d) TEM image of the WS_2 layers lying perpendicular to the electron beam direction. The inset is a zoomed image of the boxed area. The atoms in the area are highly disordered.

beam). A hexagonal atomic arrangement is easily noticed at the top right of the image, as found in other previous TEM studies.[4a] The hexagonal lattice appears to be greatly disturbed in many examined areas like in the boxed area of **Figure 4d**. Its zoomed image (the inset) shows that the atoms in the area are severely disordered. Such disordering and incomplete formation of layers, as well as the severe curling of the layer filaments, might be the reasons for the *c*-axis expansion

found from the powder pattern. We suspect that this poor crystallinity is ultimately caused by the low diffusion rate of atoms under the low-temperature reaction condition.

In a sense, the nanostructures in our WS_2 product resemble the nano filaments of WS_2 or MoS_2 catalysts that form on the surface of Al_2O_3 support. In their structures, the sulfide layers are usually deformed severely by the surface shape of the support.[35] The difference is that our sulfidation method provided such deformed nanostructures without additional heterogeneous components for the morphosynthesis, and the product is completely free from any other minerals. In any event, the lager c-spacing, high surface area and open structure of our nanoparticles should be desirable features for the applications such as lithium-batteries and catalysis. This is the opposite to the case of the fullerene-like or nanotubular structures of WS_2 and MoS_2 for which lithium intercalation could not be completed presumably because of the closed nature of those structures.[33] It is emphasized that our simple reaction scheme and setup could be a great advantage when large-scale production is considered.

(3) Preparation of TiS_2 nanoparticles and nanorods from TiO_2 nanoparticles.

The corrosive reaction of boron sulfides toward silica reaction containers at high temperatures implies that it might be possible to utilize them to sulfidize transition-metal oxides. The absence of transition-metal thioborates is also a desirable feature to avoid unwanted inclusion of boron. As boron sulfides react with metal oxides, it is anticipated that the oxide ions become substituted by sulfide ions, and that the corresponding metal sulfides form as a final product along with boron oxide (B_2O_3) as a byproduct (metathesis). B_2O_3 is soluble in water or in alcohol, and can be washed out after the sulfidation reactions. It is particularly interesting to us to examine this synthetic possibilities at the temperature region much below the melting or peritectic point of transition-metal sulfides, especially for the preparation of nanostructured metal sulfides. That is, the limited diffusion of ions during the sulfidation process may allow us to convert the oxide nanoparticles into the corresponding sulfide nanoparticles without undergoing significant fusion among them. It is emphasized that many metal oxide nanoparticles are readily available via various synthetic routes, and often commercially.

Our ongoing experiments in this project mainly focus on the preparation of nanostructured TiS_2, which was motivated by the commercial availability of TiO_2 nanoparticles in various sizes and by its technological importance. The layered structure of TiS_2 makes the compound suitable for use as high-temperature lubricants,[36] and electrode materials for high-density lithium batteries.[37] For the battery applications, it has been well established that the limitations in the rate capabilities of Li-ion batteries can be caused by slow solid-state diffusion of Li^+ within the electrode materials, and as a result, there is tremendous current research interest in the development of nanostructured Li-ion battery electrodes.[38] Despite the technological implications, it is scarce to find nanostructured TiS_2 materials in the literature with one notable exception to our knowledge. Thin films of TiS_2 in nano-thickness have been deposited via a chemical vapor deposition (CVD) route on the surface of metal microtubules as templates to obtain very high surface area.[39] The nanostructured electrode showed dramatically improved rate capabilities relative to thin-film control electrodes composed of the same material.

In the previous kinetic studies of conventional H_2S sulfidation reactions, the sulfidation of TiO_2 nanoporous materials were found to occur slowly for the internal Ti atoms even at 500

°C, and only the Ti atoms on the surface (surface area = 120 m^2/g) could be completely sulfidized to TiS_2 at 400 °C.[40] Therefore, our sulfidation reactions were attempted below 500°C in order to examine the sulfidizing activity of boron sulfides at *lower* temperatures. Nanoparticles of anatase TiO_2 with an average diameter of 32 nm[41] were loaded together with boron and sulfur powders at two different ratios (3:4:6 and 3:2:6), and heated at several different temperatures up to 450 °C. The 3:4:6 ratio corresponds to the stoichiometric reaction between TiO_2 and B_2S_3:

$$3TiO_2 + 4B + 6S \rightarrow 3TiO_2 + 2B_2S_3 \rightarrow 3TiS_2 + 2B_2O_3.$$

In addition, 325-mesh microparticles of anatase TiO_2 were also tested to compare their reactivities and reaction conditions with the nanoparticles. No sulfidation occurred up to 250 °C in any cases. Sulfidation of the TiO_2 nanoparticles took place in the reactions at 300, 350, 400 and 450 °C, and yet only at 450 °C the reactions proceeded at a significant rate, with less than ~10 % of TiO_2 nanoparticles unreacted after 18 hours for the 3:4:6 ratio reaction. The product was a mixture of ~80 % TiS_2 and ~20 % TiS_3 based on the X-ray powder diffraction pattern. It is suspected that the incomplete conversion into TiS_2 and the existence of a small amount of TiS_3 is because of incomplete reduction of sulfur by boron, and TiO_2 might have undergone the sulfidation in a sulfur-rich condition. The dark brown color of the product, the same as that of boron, is consistent with this possibility. With the 2:6 ratio of boron and sulfur, only TiS_3 was found in the product at the same reaction temperature. In any case, no boron compounds were detected, while vitreous B_2O_3 should exist in the products, although not detectable by the X-ray powder diffraction. It was also noted that the product composition also depends on the particle size of TiO_2. That is, the 325-mesh powder turned only into TiS_3 under the same reaction condition that provided ~80 % TiS_2 when the 32-nm particles were used.

Figures 5a and **5b** show the TEM images of the sample from the reaction that provided the highest yield of TiS_2. The image in **Figure 5a** exhibits a nanorod ~120 nm wide and > 3 μm long, and nanoparticles of < 90 nm in diameter. A closer look at the nanoparticles indicates that the particles are made of much smaller nanoparticles (< 40 nm) that are glued together by an amorphous material (**Figure 5b**). The chemical nature of the amorphous material is not clear yet, but it could be the B_2O_3 that was not completely dissolved in water. The nanorod in **Figure 5a** is also partly covered by a similar amorphous material. The fringes that appear in **Figure 5b** are separated by ~5.7 Å which is close to the layer distance (5.695 Å) in the bulk structure of TiS_2.[42] A totally unexpected, and yet very interesting feature is the nanorods that were found in a significant amount in the TEM sample. The electron diffraction pattern of the nanorod in **Figure 5a** shows its remarkable single crystallinity (the inset). The hexagonal Laue symmetry and the calculated unit cell parameters prove that the nanorod is indeed a single crystal of TiS_2. Both the anatase and rutile structures of TiO_2 exhibit a tetragonal symmetry.

The presence of the TiS_2 nanorods in the reaction product indicates that nanoparticles fuse together during or after the sulfidation process. Optimization of the reaction conditions may allow us to selectively prepare the nanoparticles and nanorods in the future. It is noted that B_2S_3 was prepared *in situ* so far in our reactions, and this required the reaction temperature not lower than 300 °C. It might be possible to lower the reaction temperatures by preparing B_2S_3 first *ex situ*.[43] and our recent results show that sulfidation is possible even at 200 °C for the surface Ti

atoms in the TiO_2 nanoparticles. We are also currently testing the sulfidation method on much smaller TiO_2 nanoparticles (15 nm).[44]

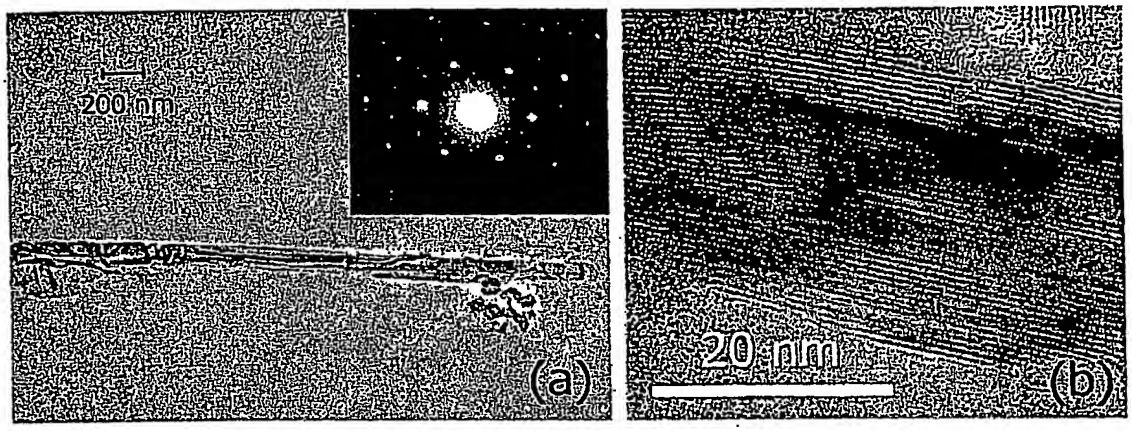

Figure 5. (a) TEM image of a nanorod and nanoparticles of TiS_2 prepared at 450 °C from TiO_2 (anatase) nanoparticles. The electron diffraction pattern of the nanorod reflects the trigonal symmetry of TiS_2 layers (inset). Both anatase and rutile structures of TiO_2 have tetragonal unit cells. (b) TEM image of a small cluster embedded in one of the nanoparticles shown in Figure 5a. The fringes correspond to individual layers of TiS_2, based on their spacing (~5.7Å).

III. Research plan

The forgoing results clearly demonstrate the viability of our new low-temperature sulfidation method that utilizes boron sulfides. The extent to which the method can be applied to other metals and metal oxides remains to be tested, and yet the underlying reaction mechanism needs to be revealed for better-controlled syntheses. For instance, it is not certain how the boron ions help the sulfidation processes when the boron sulfide vapor attacks metals or metal oxides. For metal oxides, it will be also important to understand how the formation of boron oxide affects the size and morphology of the nanostructures during the reactions.

Answering all the relevant questions would be of course our ultimate goal, as well as characterization of the chemical and physical properties of our target nanostructured materials. During this funding period, however, we will focus on the first question, and explore the limits and possibilities of our new sulfidation method from the synthetic point of view. First, as a continuation of our forgoing experiments, we seek to synthesize nanowires, nanorods and nanoparticles of various transition-metal sulfides via sulfidation of metals and metal oxides. Second, we will develop other methodologies to achieve sulfidation reactions in organic media, thereby further lowering the reaction temperatures. The success of the proposed work will provide unprecedented nanostructures of transition-metal sulfides via establishment of systematic reaction conditions for the control of the size and morphology, and via characterization of the morphology and surfaces of the materials. In the following sections, we describe the detailed plans of our proposed research.

(1) Controlled reactions for nanowires of TaS_3.

The intriguing features of our ultralong TaS_3 nanowires would be, first, they are quiasi-1D conductors with CDW properties, and second, they grow from the surfaces of the mother metal pieces, thereby having a *natural* electrical contact with a larger conducting object. The electrical behavior of 1D electronic systems has been an active research topic, and TaS_3 nanowires can provide an interesting test ground for many theoretical concepts such as Luttinger liquid,[45] Wigner crystal[46] and quantum nucleation,[47] because its electronic structure inherently exhibits effects associated with reduced dimensionality in addition to the morphological 1D character. Recent studies showed that the size effect appears even for the samples in (sub)micron scale.[26, 48] We anticipate that our new TaS_3 nanowires will provide more interesting observations in the extreme regime of 1D anisotropy. Chemical aspects of the TaS_3 nanowires cannot be ignored, either. The high surface area and the natural electrical contact should allow us to readily explore possible applications of the materials as nanoelectrodes for batteries and electrochemical storage of H_2, or chemical sensors. It may be also possible to use them to connect metal nanoparticles in the fabrication of nanodevices.

For the applications of TaS_3 nanowires, it is essential to establish a standard procedure to grow them in a controlled manner, and during the funding period we will seek to achieve that. Unfortunately, the thermodynamic information on boron sulfides is quite limited, and hence right at this moment it will not be possible to control the partial pressures of boron sulfides and sulfur in a precise manner. However, our experiences show that certain compositions of boron sulfides and reaction temperatures are particularly preferable to obtain wires with smaller cross section areas. The shape of Ta metal pieces and their distance from the liquid boron sulfides at the bottom of the container also seem to affect the wire lengths. As an extension of our research, we will also use alloys, for example, $Ta_{1-x}M_x$ (M = Nb, Zr, Hf, Mo, W), to prepare doped TaS_3 nanowires, in order to change the electron concentration or the valence band structure. Such optimizations of the electronic characteristics might lead to enhanced properties for (electro)chemical applications. Alloys can be easily prepared by arcmelting proper amounts of the metals.

(2) Preparation of tungsten and molybdenum sulfide catalysts without supports.

Compounds containing sulfur and nitrogen in crude oil contribute to the air pollution by formation of acid rain and photosmog in the form of SO_2 and NO_x, and it becomes increasingly important to improve the performance of the hydrotreating catalysts to lower the sulfur and nitrogen contents in fuels.[49, 50] The catalysts used in hydrodesulfurization are MoS_2 and WS_2 phases supported on alumina (Al_2O_3) to which nickel or cobalt are added as promoters.[50a, b] These catalysts are most frequently prepared by the impregnation of a support with solutions of salts of the corresponding metals.[50a, b] The catalyst performance depends on the nature of the support, its chemical and phase composition, the surface structure and texture, and the shape and size of the support granules.[50c] At least twelve models of the active component of the hydrodesulfurization catalysts have been proposed, which indicates the complicated nature of the studies of those catalysts.[35, 50, 51] A primary difference among the models is the location and chemical nature of the promoter element, Ni or Co, in the catalyst particles. For example, a contact synergism model for Co-Mo-S catalysts suggest the existence of small particles of Co_9S_8 in contact with MoS_2 nanocrystals.[51k, l] In another widely cited model, the promoter elements

exist predominantly at "edge" sites around the waist of the cylinder surface of the nanocrystals (**Figure 6**).[51m]

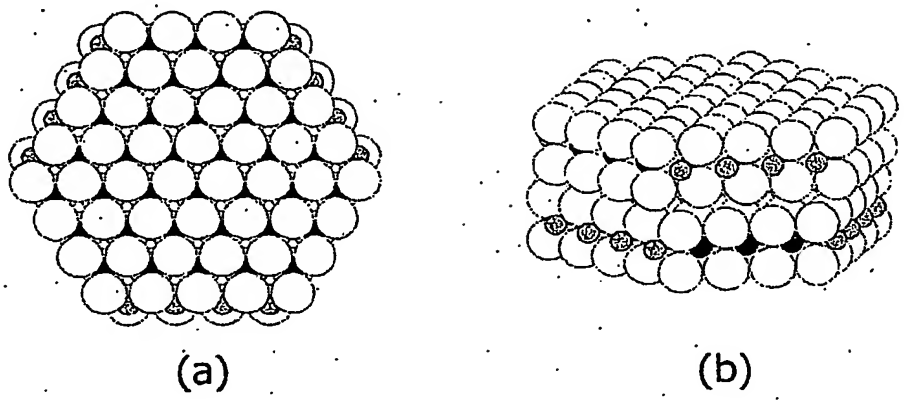

Figure 6. Idealized model for a possible structure of Co-Mo-S catalysts with two truncated layers. (a) [001] and (b) ~[110] projection views. Small black, small gray and large light gray atoms represent Mo, Co and S atoms, respectively. Co atoms terminate three edges of a hexagonally-truncated layer, and are exposed to the surrounding environment.

Based on our successful preparation of WS_2 nanostructures by direct sulfidation of tungsten metal, it is our interest to sulfidize the alloys of Co (or Ni) and Mo (or W). When Co-Mo alloys, for example, form sulfides in a *low-temperature* reaction condition, the Co and Mo atoms will redistribute themselves, and eventually the two different metal elements might become separated from each other instead of forming their bimetallic sulfides due to a high activation barrier (see the next section). The diffusion rate of Co atoms should be very important in determining the size of MoS_2 particles; i.e., a very slow diffusion of the Co atoms through the sulfide lattice may prevent MoS_2 crystals from growing into larger sizes, and the resultant nanostructures of MoS_2 could be much smaller than those found from our previous sulfidation of "pure" molybdenum. The original content of Co in the alloys can be also a governing factor. For example, the ratio of Co and Mo in the nanocrystallite shown in **Figure 6** is 1:3. An alloy with a higher Co content may provide smaller crystallites, if all the Co atoms are to be the terminating atoms. Certainly, detection of such terminal atoms could be challenging, and yet Center for High resolution Microscopy at ASU is suitable for such a task, being capable of EELS elemental analysis within 2.0 Å resolution.

It is also noted that our sulfidation process does not require a support such as alumina, and hence the expected nanoparticles are support-free. This could be helpful to study the effect of the particle-substrate interactions on the shape and morphology of the catalyst nanocrystallites. Furthermore, whether Co_9S_8 clusters form and have a physical contact with MoS_2 particles might be easily verified in TEM studies on our product, simply because there are no other places the clusters can be anchored except the surfaces of MoS_2 particles. The interference by support atoms in TEM studies no longer exist, either.[52] We emphasize that in principle the sulfidation of metal alloys can be extended for other bimetallic sulfide nanostructures.

(3) Preparation of nanostructures of binary and ternary transition-metal sulfides from their oxides.

A natural extension of our preparation of TiS_2 nanostructures will be the application of the method to other metal oxides. Although not presented here, our preliminary experiments showed that $BaTiO_3$ microparticles could be converted into $BaTiS_3$ in a high yield at 450 °C with no visible fusion of the particles. The detailed analysis of the product is in progress, and the reactions will also be carried out for nanoparticles of $BaTiO_3$. It is noted that in the literature there have been no reports on nanostructured *ternary* transition-metal sulfides, to our knowledge.

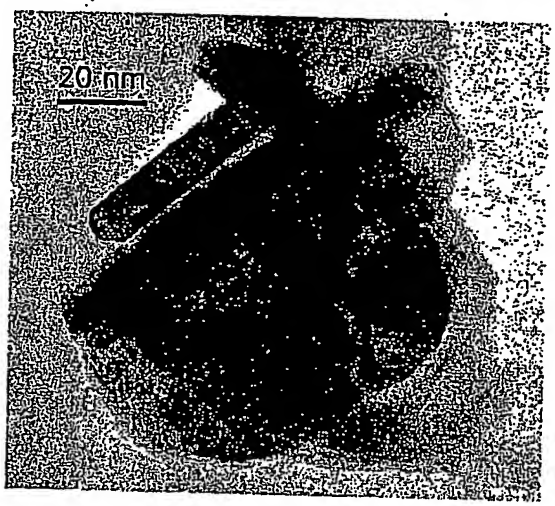

Figure 7. TEM image of NbS_2 nanoparticles. Particles are stacked along the beam axis in the lower part of the image.

In one of our other preliminary reactions, Nd_2O_3 (49 – 64 nm)[53] was completely sulfidized into NdS_2 at 450 °C in a day, and the color of the powder turned into grayish yellow from pale violet. We recognize that the product is not Nd_2S_3, the corresponding sulfide of Nd_2O_3, and this can be attributed to an incomplete reaction between boron and sulfur. The product was examined under a TEM microscope after dispersed in deionized water, and was found to generally maintain the original sizes after the sulfidation, as found in the TEM image in **Figure 7**. Although not shown here, the fringes and atomic spacing in the images are in a good agreement with the reported crystallographic data of NdS_2.[54] The particles appear to have a shape of thin disks. To our knowledge, the only rare-earth sulfide nanostructure reported in the literature to date is EuS nanoparticles that show an interesting luminescent characteristic.[55]

Application of the method to WO_3 and MoO_3 should be interesting. The current large-scale synthesis of fullerene-like and nanotubular structures of WS_2 and MoS_2 is carried out by sulfidation of WO_3 and MoO_3 at high temperatures, and it has been argued that the high temperature condition is necessary for the initial formation of curled layers.[2b] Our low temperature sulfidation will allow us to examine the assertion in different reaction conditions.[2e] In addition, we will seek to prepare nanoparticles of magnetic sulfides such as chromium and gadolinium sulfides for possible applications in ferrofluids as well as for fundamental studies of nanomagnetics. Amorphous binary sulfides such as CrS_3 are also of our interest.[56]

One intriguing situation arises when a ternary oxide compound does not have its corresponding sulfide with the same stoichiometry. For example, there does not exist $FeSiS_3$ while $FeSiO_3$ can be easily prepared by solid state reactions under pressure.[57] The only ternary sulfide in the Fe-Si-S system is Fe_2SiS_4. Under a low-temperature condition in which the diffusion of atoms is rather limited, sulfidation of $FeSiO_3$ may not provide Fe_2SiS_4 crystallites. It

is because the low temperature reaction condition is unlikely to provide enough energy to overcome the thermal activation barrier to form a new ternary phase. Instead, as found in our experiments, the $FeSiS_3$ became completely decomposed into binary sulfides, FeS_2 and SiS_2, during the sulfidation process (destructive sulfidation). Interestingly, the starting material was microcrystalline, but the product seemed to be nanostructured. For example, the volume of the reaction mixture increased by about six times, and the product was a much finer and floppy powder. SiS_2 is reactive to water, and we could remove it along with boron sulfides by washing the product in deionized water. The X-ray powder pattern shows a pure phase of FeS_2. The preliminary SEM studies on the sample indicated that the size of the product powder was smaller than the resolution limit of our instrument, and TEM studies are under way. FeS_2 is a well-known battery material, and exhibits interesting quantum confinement effect when the size is smaller than 10 nm.[11b] The overall implication is that by carefully selecting ternary oxides, we might be able to prepare nanoparticles of binary sulfides by destructive sulfidation of the ternary oxides that are much larger in particle size. Sulfidation of $Mo_3Al_2O_{12}$ and $TiAl_2O_5$ (prepared under ambient pressure) is currently being examined because Al_2S_3 is easily dissolved in water by forming aluminum hydroxides.

(4) Other new methodologies employing boron sulfides as a sulfidizing agent.

Boron sulfides exist as a solid at room temperature, while other sulfidizing agents such as H_2S and CS_2 are either a gas or a liquid with a very low boiling point. Therefore, B_2S_3 can be introduced much more conveniently into organic solvents in which the sulfidation reaction can take place. The advantages of such inorganic reactions in an organic medium are (1) reaction temperatures can be lowered even more, and (2) the particles are well separated and dispersed to avoid or control their possible fusion. By optimizing the reaction conditions, we might be able to sulfidize only the surfaces of metal or metal oxide nanoparticles until the outer sulfide shell reaches to a desired thickness. It might be also possible to prepare nanoparticles that contain both oxide and sulfide well mixed together in individual particles. Photocatalytic activities have been reported for mixed WO_3/WS_2, although neither of the binary compounds is known as a photocatalyst.[58]

One simple reaction scheme that we will exploit in this project is simple reflux of organic medium in which metal or oxide nanoparticles are put together with B_2S_3. Such reactions have been employed in some organic and organometallic reactions. For example, terminal oxygen atoms in thiapendione could be replaced by sulfur atoms on treatment of B_2S_3 in refluxing toluene.[13a] Reaction of vanadyl complexes with excess B_2S_3 in refluxing CH_2Cl_2 provided thiovanadyl complexes with no indication of attack on other coordinated ligands.[13b] More recently, the reaction of Tp^*WO_2Cl with B_2S_3 in refluxing 1,2-dichloroethane produced its sulfidated analogues.[13c] Instead of organic or organometallic molecules, we seek to sulfidize oxide nanoparticles that are suspended in refluxing organic media. Certainly, the small size of nanoparticles should be advantageous under low temperature conditions in which the diffusion of atoms is slow. We are currently working on controlled sulfidation of TiO_2 nanoparticles (ca. 12 nm) in various refluxing organic solvents. It would be also viable to use other compounds as starting materials: e.g., $TiCl_4$ or $Ti(OR)_4$ (R = alkyl) to obtain TiS_2.[59] It also remains to be seen whether we can utilize additional reaction agents, such as $LiAlH_4$ or CaH_2, to provide a reducing environment. This is analogous to the use of H_2/H_2S mixture in conventional sulfidation process.

REFERENCES AND NOTES

1. See for example, (a) *Sulfur. Its Significance for Chemistry, for the Geo-, Bio- and Cosmosphere and Technology*; Müller, A.; Krebs, B., Eds., Elsevier; Amsterdam, 1984. (b) *Transition Metal Sulfur Chemistry; Biological and Industrial Significance*; Stiefel, E. I., Matsumoto, K., Eds.; ACS Symposium Sereis 535; American Chemical Society: Washington D. C., 1996.
2. (a) Tenne, R.; Margulis L.; Genut, M.; Hodes, G. "Polyhedral and cylindrical structures of tungsten disulphide," *Nature (London)* **1992**, *360*, 444. (b) Feldman, Y.; Wasserman, E.; Srolovitz, D. J.; Tenne, R. "High-rate, gas-phase growth of MoS_2 nested inorganic fullerenes and nanotubes," *Science (Washington, D. C.)* **1995**, *267*, 222. (c) Chhowalla, M.; Amaratunga, G. A. J. "Thin films of fullerene-like MoS_2 nanoparticles with ultra-low friction and wear," *Nature (London)* **2000**, *407*, 164. (d) Rothschild, A.; Sloan, J.; Tenne, R. "Growth of WS_2 nanotubes phases," *J. Am. Chem. Soc.* **2000**, *122*, 5169. (e) Whitby, R. L. D.; Hsu, W. K.; Kroto, H. W.; Walton, D. R. M. "Conversion of amorphous WO_{3-x} into WS_2 nanotubes," *Phys. Chem. Chem. Phys.* **2002**, *4*, 3938.
3. Zelenski, C. M.; Dorhout, P. K. "Template synthesis of near-monodisperse microscale nanofibers and nanotubles of MoS_2," *J. Am. Chem. Soc.* **1998**, *120*, 734.
4. (a) José-Yacamán, M.; Lopez, H.; Santiago, P.; Galvan, D. H.; Garzón, I. L.; Reyes, A. "Studies of MoS_2 structures produced by electron irradiation," *Appl. Phys. Lett.* **1996**, *69*, 1065. (b) Homyonfer, M.; Mastai, Y.; Hershfinkel, M.; Volterra, V.; Hutchison, J. L.; Tenne, R. "Scanning tunneling microscope induced crystallization of fullerene-like MoS_2," *J. Am. Chem. Soc.* **1996**, *118*, 7804.
5. (a) Mdleleni, M. M.; Hyeon, T.; Suslick, K. S. "Sonochemical synthesis of nanostructured molybdenum sulfide," *J. Am. Chem. Soc.* **1998**, *120*, 6189. (b) Mastai, Y.; Homyonfer, M.; Gedanken, A.; Hodes, G. "Room temperature sonoelectrochemical synthesis of molybdenum sulfide fullerene-Like nanoparticles," *Adv. Mater.* **1999**, *11*, 1010.
6. Albu-Yaron, A.; Levy-Clement, C.; Hutchison, J. L. "A study on MoS_2 thin films electrochemically deposited in ethylene glycol at 165 °C," *Electrochem. Solid-State Lett.* **1999**, *2*, 627. The as-deposited sample was amorphous, and showed some crystallinity after annealed at 550 °C for 1 hr. However, the HRTEM images indicated the existence of a large amount of the amorphous phases even after the annealing.
7. (a) Wilcoxon, J. P.; Samara, G. A. "Strong quantum-size effects in a layered semiconductor: MoS_2 nanoclusters," *Phys. Rev. B* **1995**, *51*, 7299. (b) Parsapour, F.; Kelley, D. F.; Craft, S.; Wilcoxon, J. P. "Electron transfer dynamics in MoS_2 nanoclusters: normal and inverted behavior," *J. Chem. Phys.* **1996**, *104*, 4978. (c) Wilcoxon, J. P.; Newcomer, P. P.; Samara, G. A. "Synthesis and optical properties of MoS_2 and isomorphous nanoclusters in the quantum confinement regime," *J. Appl. Phys.* **1997**, *81*, 7934. (d) Thurston, T. R.; Wilcoxon, J. P. "Photooxidation of organic chemicals catalyzed by nanoscale MoS_2," *J. Phys. Chem. B* **1999**, *103*, 11.
8. Duphil, D.; Bastide, S.; Lévy-Clément, C. "Chemical synthesis of molybdenum disulfide nanoparticles in an organic solution," *J. Mater. Chem.* **2002**, *12*, 2430. The as-prepared sample was amorphous, and showed some crystallinity after annealed at 550 °C for 1 hr.
9. Nath, M.; Rao, C. N. R. "New metal disulfide nanotubes," *J. Am. Chem. Soc.* **2001**, *123*, 4841.
10. (a) Zhu, Y. Q.; Hsu, W. K.; Kroto, H. W.; Walton, D. R. M. "Carbon nanotube template promoted growth of NbS_2 nanotubes/nanorods," *Chem. Commun.* **2001**, *1*, 2184. (b) Whitby,

R. L. D.; Hsu, W. K.; Boothroyd, C. B.; Kroto, H. W.; Walton, D. R. M. "Tungsten disulphide coated multi-walled carbon nanotubes," *Chem. Phys. Lett.* **2002**, *359*, 121. (c) Brorson, M.; Hansen, T. W.; Jacobsen, C. J. H. "Rhenium(IV) sulfide nanotubes, *J. Am. Chem. Soc.* **2002**, *124*, 11582.

11. (a) Martino, A.; Wilcoxon, J. P.; Kawola, J. S. "Synthesis and characterization of coal liquefaction catalysts in inverse micelles," *Energy & Fuels* **1994**, *8*, 1289. (b) Wilcoxon, J. P.; Newcomer, P. P.; Samara, G. A. "Strong quantum confinement effects in semiconductors: FeS_2 nanoclusters," *Solid State Commun.* **1996**, *98*, 581.
12. Lu, Q.; Hu, J.; Tang, K.; Qian, Y.; Liu, X.; Zhou, G. "A simple method for the preparation of nanocrystalline transition metal sulfides," *J. Solid State Chem.* **1999**, *146*, 484.
13. (a) Schumaker, R. R.; Engler, E. M. "Thiapen chemistry. 2. synthesis of 1,3,4,6-tetrathiapentalene-2,5-dione," *J. Am. Chem. Soc.* **1977**, *99*, 5521. (b) Callahan, K. P.; Durand, P. J. "Reactions of the vanadyl group: synthesis of $V{=}S^{2+}$ and VBr_2^{2+} from $V{=}O^{2+}$ complexes," *Inorg. Chem.* **1980**, *19*, 3211. (c) Eagle, A. A.; Tiekink, E. R. T.; George, G. N.; Young, C. G. "Synthesis, characterization, and electrochemistry of *cis*-oxothio- and cis-bis(thio)tungsten(VI) complexes of hydrotris(3,5-dimethylpyrazol-1-yl)borate," *Inorg. Chem.* **2001**, *40*, 4563.
14. See for example, (a) Krebs, B. "Thio- and selenoborates: from rings to clusters and networks," *Phosphorus, Sulfur and Silicon and the Related Elements* **2001**, *168*. 11 and references therein. (b) Conrad, Olaf; Jansen, Christoph; Krebs, Bernt. "Boron-sulfur and boron-selenium compounds - From unique molecular structural principles to novel polymeric materials," *Angew. Chem, Intern. Ed.* **1998**, *37*, 3209 and references therein. (c) Martin, S. W.; Cho, J.; Polewik, T.; Bhowmik, S. "Density of $x Na_2S{\cdot}(1\text{-}x)B_2S_3$ ($x = 0$ to 0.8) glasses: correlation with short-range order," *J. Am. Ceram. Soc.* **1995**, *78*, 3329. (d) Cho, J.; Martin, S. W. "Infrared spectra of lithium thioborate glasses and polycrystals," *J. Non-Cryst. Solids* **1994**, *170*, 182. (e) Kincs, J.; Cho, J.; Bloyer, D.; Martin, S. W. "Glass transition and heat capacities of inorganic glasses: Diminishing change in the heat capacity at T_g for $x Na_2S + (1{-}x)B_2S_3$ glasses," ASTM Special Technical Publication 1994, STP 1249(Assignment of the Glass Transition), 185. (f) Cho, J.; Martin, S. W. "Infrared spectroscopy of glasses and polycrystals in the series $x Cs_2S + (1\text{-}x)B_2S_3$," *J. Non-Cryst. Solids* **2002**, *298*, 176.
15. *Chemistry of the elements*, Greenwood, N. N.; Earnshaw, A.; Pergamon Press: Oxford, 1984.
16. *Ullmann's Encyclopedia of industrial chemistry, Vol A4*, Gerhartz, W.; Yamamoto, Y. S.; Campbell, F. T.; Pfefferkorn, R.; Rounsaville, J. F. Eds. VCH Publishers: Weinheim, 1985, p315
17. *Inorganic crystal structure database (ICSD)*; Fachinformationszentrum-Karlsruhe, Germany, 2001.
18. (a) Thomas, D.; Tridot, G. "Preparation and study of a double sulfide of boron and manganese," *Compt. Rend.* **1964**, *258*, 2587. (b) Kimmerle, F. M.; Giasson, G. "Cathode reactants in high-energy density aprotic battery systems, Metallic borosulfides," *J. Electrochem. Soc.* **1973**, *120*, 1214.
19. Hagenmuller, P.; Perez, G.; Serment, J.; Hardy, A. "Manganese orthothiosilicate and orthothiogermanate," *Compt. Rend.* **1964**, *259*, 4689.
20. See for example, (a) Coste, S.; Kopnin, E.; Evain, M.; Jobic, S.; Brec, R.; Chondroudis, K.; Kanatzidis, M. G. "Polychalcogenophosphate flux synthesis of 1D-$KInP_2Se_6$ and 1D and 3D-$NaCrP_2S_6$," *Solid State Sci.* **2002**, *4*, 709. (b) Derstroff, V.; Ensling, J.; Ksenofontov, V.; Gutlich, P.; Tremel, W. $K_3Cr_2(PS_4)_3$: a new chromium thiophosphate with a one-dimensional $[Cr_2(PS_4)_3]^{3-}$ anion chain.," *Z. Anorg. Allg. Chem.* **2002**, *628*, 1346. (c) Woo, A. J.; Kim, S.-J.;

Park, Y. S.; Goh, E.-Y. "The 31P NMR chemical shielding tensors in quaternary metal thiophosphates, $NaNb_2PS_{10}$, $AgNb_2PS_{10}$, $Au_{0.5}Nb_2PS_{10}$, and $NaSmP_2S_6$," *Chem. Mater.* **2002**, *14*, 518. (d) Coste, S.; Kopnin, E.; Evain, M.; Jobic, S.; Payen, C.; Brec, R. "$Na_3Cr_2P_3S_{12}$ and $K_3Cr_2P_3S_{12}$: Two new one-dimensional thiophosphate compounds with a novel structure," *J. Solid State Chem.* **2001**, *162*, 195. (e) Huang, Z.-L.; Zhao, J.-T.; Mi, J.-X.; Mao, S.-Y.; Zheng, L.-S. "Room temperature solid state synthesis and characterization of a new chromium thiophosphate $Cr_4(P_2S_6)_3$," *J. Solid State Chem.* **1999**, *144*, 388. (f) Evans, J. S. O.; O'Hare, D.; Clement, R.; Leaustic, A.; Thuery, P. "Origins of the spontaneous magnetization in $MnPS_3$ intercalates: a magnetic susceptibility and powder neutron diffraction study," *Adv. Mater.* **1995**, *7*, 735.

21. Meerschaut, A.; Guemas, L.; Rouxel, J. "Etude structurale du trisulfure de tantale," *Comp. Rend. Serie C*, **1980**, *290*, 215.
22. See for example, (a) Sambongi, T.; Tsutsumi, K.; Shiozaki, Y.; Yamamoto, M.; Yamaya, K.; Abe, Y. "Peierls transition in tantalum trisulfides," *Solid State Commun.* **1977**, *22*, 729. (b) Haen, P.; Mignot, J. M.; Monceau, P.; Nunez-Regueiro, M.; Richard, J. "Transport properties in transition metal trichalcogenides," *Lect. Notes Phys.* **1979**, *95*, 323. (c) Sambongi, T.; Ido, M.; Tsutsumi, K.; Yamamoto, M.; Takoshima, T.; Abe, Y. "Phase transitions and electric properties of MX_3," *Lect. Notes Phys.* **1979**, *95*, 349. (d) Thompson, A. H.; Zettl, A.; Gruener, G. "Charge-density-wave transport in tantalum sulfide (TaS_3)," *Phys. Rev. Lett.* **1981**, *47*, 64. (e) Zettl, A.; Gruener, G. "Charge-density-wave dynamics in tantalum sulfide (TaS_3)," *Phys. Rev. B.* **1982**, *25*, 2081. (f) Miller, J. H., Jr.; Richard, J.; Tucker, J. R.; Bardeen, J. "Evidence for tunneling of charge-density waves in tantalum sulfide (TaS_3)," *Phys. Rev. Lett.* **1983**, *51*, 159.
23. Roucau, C.; Ayroles, R.; Monceau, P.; Guemas, L.; Meerschaft, A.; Rouxel, J. "Electron diffraction and resistivity measurements on the one-dimensional orthorhombic and monoclinic structures of TaS_3. Comparision with $NbSe_3$," *Phys. Sta. Sol. (A)* **1980**, *62*, 483.
24. Narang, S. C.; Ventura, S. C.; Cox, P. "Ion battery using high aspect ratio electrodes," PCT Int. Appl. 1999, US 97-68764.
25. Broadhead, J.; DiSalvo, F. J., Jr.; Trumbore, F. A. "Nonaqueous battery using chalcogenide electrode," U.S. (1975), US 73-352514
26. Van der Zant, H. S. J.; Slot, E.; Zaitsev-Zotov, S. V.; Artemenko, S. N. "Negative resistance and local charge-density-wave dynamics," *Phys. Rev. Lett.* 2001, 87, 126401.
27. (a) Tanda, S.; Tsuneta, T.; Okajima, Y.; Inagaki, K.; Yamaya, K.; Hatakenaka, N. "Crystal topology: A Moebius strip of single crystals," *Nature (London)* **2002**, *417*, 397. (b) Tanda, S.; Sajiki, K.; Tsuneta, T.; Okajima, Y.; Yamaya, K. "Manufacture of crystalline rings from chalcogenides by droplet evaporation on a substrate," U.S. Pat. Appl. Publ. 2002, US 2001-939450.
28. Meerschaut, A.;Guemas, L.;Rouxel, J. "Structure and properties of the new phase of the pseudo one-dimensional compound TaS_3," *J. Solid State Chem.* **1981**, *36*, 118.
29. Canadell, E.; Rachidi, I. E. I.; Pouget, J. P.; Gressier, P.; Meerschaut, A.; Rouxel, J.; Jung, D.; Evain, M.; Whangbo, M.-H. "Comparison of the electronic structures of layered transition-metal trichalcogenides thallium triselenide, thallium trisulfide and niobium triselenide," *Inorg. Chem.* **1990**, *29*, 1401.
30. Van der Vlies, A. J.; Prins, R.; Weber, Th. "Chemical principles of the sulfidation of tungsten oxides," *J. Phys. Chem. B* **2002**, *106*, 9277.

31. The superior lubricating properties of inorganic-fullerene WS_2 (120 nm in diamter) has been demonstrated in comparison to *micro-sized, not nano-sized,* 2H-WS_2 with the average size of 4μm. Our large-scale production of new plate-like nanostructures of pure WS_2, which is described in this section, will finally allow a realistic comparison of lubricating properties between spherical and plate-like nanostructures in practical applications. For the friction studies on the hollow inorganic-fullerene WS_2 nanoparticles, see for example, (a) Rapoport, L.; Bilik, Y.; Feldman, Y.; Homyonfer, M.; Cohen, S. R.; Tenne, R. "Hollow nanoparticles of WS_2 as potential solid-state lubricants," *Nature (London)* **1997**, *387*, 791. (b) Rapoport, L.; Feldman, Y.; Homyonfer, M.; Cohen, H.; Sloan, J.; Hutchison, J. L.; Tenne, R. "Inorganic fullerene-like material as additives to lubricants: structure-function relationship," *Wear* **1999**, *225-229(Pt. 2)*, 975. (c) Golan, Y.; Drummond, C.; Homyonfer, M.; Feldman, Y.; Tenne, R.; Israelachvili, J. "Microtribology and direct force measurement of WS_2 nested fullerene-like nanostructures," *Adv. Mater.* **1999**, 11, 934. (d) Rapoport, L.; Lvovsky, M.; Lapsker, I.; Leshchinsky, W.; Volovik, Y.; Feldman, Y.; Tenne, R. "Friction and wear of bronze powder composites including fullerene-like WS_2 nanoparticles," *Wear* **2001**, 249, 150. (e) Rapoport, L.; Lvovsky, M.; Lapsker, I.; Leshinsky, V.; Volovik, Y.; Feldman, Y.; Zak, A.; Tenne, R. "Slow release of fullerene-like WS_2 nanoparticles as a superior solid lubrication mechanism in composite matrices," *Adv. Eng. Mater.* **2001**, *3*, 71. (f) Tenne, R.; Rapoport, L.; Lvovsky, M.; Feldman, Y.; Leshchinsky, V. "Hollow fullerene-like nanoparticles as solid lubricants in composite metal matrices," PCT Int. Appl. 2001, WO 2001-IL204. (g) Drummond, C.; Alcantar, N.; Israelachvili, J.; Tenne, R.; Golan, Y. "Microtribology and friction-induced material transfer in WS_2 nanoparticle additives," *Adv. Func. Mater.* **2001**, *11*, 348. (h) Rapoport, L.; Leshchinsky, V.; Lvovsky, M.; Lapsker, I.; Volovik, Yu; Tenne, R. "Load bearing capacity of bronze, iron and iron-nickel powder composites containing fullerene-like WS_2 nanoparticles," *Trib. Intern.* **2002**, *35*, 47. (i) Cizaire, L.; Vacher, B.; Le Mogne, T.; Martin, J. M.; Rapoport, L.; Margolin, A.; Tenne, R. "Mechanisms of ultra-low friction by hollow inorganic fullerene-like MoS_2 nanoparticles," *Surf. Coat. Tech.* **2002**, *160*, 282.

32. Schutte, W. J. ;de Boer, J. L. ;Jellinek, F. "Crystal structures of tungsten disulfide and diselenide," *J. Solid State Chem.* **1987**, *70*, 207.

33. Zak, A.; Feldman, Y.; Lyakhovitskaya, V.; Leitus, G.; Popovitz-Biro, R.; Wachtel, E.; Cohen, H.; Reich, S.; Tenne, R. "Alkali metal intercalated fullerene-like MS_2 (M = W, Mo) nanoparticles and their properties," *J. Am. Chem. Soc.* **2002**, *124*, 4747.

34. (a) Saito, Y.; Yoshikawa, T.; Bandow, S.; Tomita, M. "Interlayer spacings in carbon nanotubes," *Phys. Rev. B* **1993**, *48*, 1907. (b) Yosida, Y. "Superconducting single crystals of TaC encapsulated in carbon nanotubes," *Appl. Phys. Lett.* **1994**, *64*, 3048. (c) Li, M.; Cowley, J. M. "Structures of carbon nanotubes studied by HRTEM and nanodiffraction," *Ultramicroscopy* **1994**, *53*, 333.

35. Sharma, R.; Davis, B. H. "On the structure of a nickel-molybdenum-alumina catalyst," *Catal. Lett.* **1993**, *17*, 363.

36. Haltner, A. J.; Oliver, C. S. "Frictional properties of some solid lubricant films under high load," *J. Chem. Eng. Data* **1961**, *6*, 128

37. (a) Whittingham, M. S. "Chemistry of intercalation compounds: Metal guests in chalcogenide hosts," *Prog. Solid State Chem.* **1978**, *12*, 41. (b) Whittingham, M. S. "Electrical energy storage and intercalation chemistry," *Science (Washington, D. C.)* **1976**, *192*, 1126. (c) Murphy, D. W.; Christian, P. A. "Solid state electrodes for high energy batteries," *Science*

(Washington, D. C.) **1979**, *205*, 651. (d) *Lithium Batteries*; Gabano, J. P., Ed.; Academic Press: London, 1983.

38. For example, see Sides, C. R.; Li, N.; Patrissi, C. J.; Scrosati, B.; Martin, C. R. "Nanoscale materials for lithium-ion batteries," *MRS Bulletin* **2002**, *27*, 604.

39. (a) Che, G.; Jirage, K. B.; Fisher, E. R.; Martin, C. R.. "Chemical-vapor deposition-based template synthesis of microtubular TiS_2 battery electrodes," *J. Electrochem. Soc.* **1997**, *144*, 4296. (b) Cepak, V. M.; Hulteen, J. C.; Che, G.; Jirage, K. B.; Lakshmi, B. B.; Fisher, E. R.; Martin, C. R. "Fabrication and characterization of concentric-tubular composite micro- and nanostructures using the template-synthesis method," *J. Mater. Res.* **1998**, *13*, 3070. (c) Martin, C. R.; Mitchell, D. T. "Template-synthesized nanomaterials in electrochemistry," *Electroanal. Chem.* **1999**, *21*, 1.

40. Wang, D.; Qian, W.; Ishihara, A.; Kabe, T. "Elucidation of sulfidation state and hydrodesulfurization mechanism on TiO_2 catalysts using ^{35}S radioisotope tracer methods," *J. Catal.* **2001**, *203*, 322.

41. Alfa Aesar, Cat. No. 39953.

42. Chianelli, R. R.; Scanlon, J. C.; Thompson, A. H. "Structure refinement of stoichiometric TiS_2," *Mater. Res. Bull.* **1974**, *10*, 1379.

43. The preparation method of B_2S_3 has been well documented in the literature. See for example, Martin, S. W.; Bloyer, D. R. "Preparation of high-purity vitreous boron sulfide (B_2S_3)," *J. Am. Ceram. Soc.* **1990**, *73*, 3481.

44. Nanostructured & Amorphous Materials, Inc., Cat. No. 5430MR.

45. (a) Haldane, F. D. M. "Luttinger liquid theory of one-dimensional quantum fluids. I. Properties of the Luttinger model and their extension to the general 1D interacting spinless Fermi gas," *J. Phys. C: Solid State Phys.* **1981**, *14*, 2585. (b) Phillips, J. C. "Stretched exponential relaxation in molecular and electronic glasses," *Rep. Prog. Phys.* **1996**, *59*, 1133. (c) Zaitsev-Zotov, S. V.; Go, M. S. H.; Slot, E.; van der Zant, H. S. J. "Luttinger-liquid-like behavior in bulk crystals of the quasi-one-dimensional conductor $NbSe_3$," *Los Alamos National Laboratory, Preprint Archive, Condens. Matter* **2001**, 1, arXiv:cond-mat/0110629. http://xxx.lanl.gov/ps/cond-mat/0110629

46. (a) Schultz, H. J. "Wigner crystal in one dimension," *Phys. Rev. Lett.* **1993**, *71*, 1864. (b) Wigner, E. "The interaction of electrons in metals," *Phys. Rev.* **1934**, *46*, 1002.

47. (a) Takane, Yositake. "Quantum nucleation of phase slip in charge-density-wave systems: role of long-range Coulomb interactions," *J. Phys. Soc. Japan* **2002**, *71*, 1824. (b) Miller, J. H., Jr.; Ordonez, C.; Prodan, E. "Time-correlated soliton tunneling in charge and spin density waves," *Phys. Rev. Lett.* **2000**, *84*, 1555. (c) Matsuda, K.-I.; Tanda, S.; Shiobara, M.; Okajima, Y.; Yamaya, K.; Hatakenaka, N. "Quantum collective dynamics of charge-density waves in quasi-one-dimensional orthorhombic TaS_3," *J. Phys. Soc. Japan* **2000**, *69*, 1251. (d) Hatakenaka, N.; Shiobara, M.; Matsuda, K.-I.; Tanda, S. "Dimensional crossover of quantum nucleation processes in charge-density-wave phase slips," *Phys. Rev. B* **1998**, *57*, R2003. (e) Freire, Jose A.; Arovas, Daniel P.; Levine, Herbert. "Quantum nucleation of phase slips in a 1D model of a superfluid," *Phys. Rev. Lett.* **1997**, *79*, 5054. (f) Zaitsev-Zotov, S. V. "Classical-to-quantum crossover in charge-density wave creep at low temperatures," *Phys. Rev. Lett.* **1993**, *71*, 605. (g) Duan, J. M. "Homogeneous quantum phase slippage in bulk charge-density-wave systems," *Phys. Rev. B* **1993**, *48*, 4860.

48. Zaitsev-Zotov, S. V.; Pokrovskii, V. Ya.; Monceau, P. "Transition to one-dimensional conduction with decreasing thickness of the crystals of TaS_3 and $NbSe_3$ quasi-one-dimensional conductors," *JETP Letters* **2001**, *73*, 25.

49. See for example, *EPA Staff Paper on Gasoline Sulfur Issues*; U.S. Environmental Protection Agency. Office of Mobile Sources. U.S. Government Printing Office: Washington, D.C., 1998; EPA420-R-98-005.

50. (a) Topsøe, H.; Clausen, B. S.; Massoth, F. E. In *Hydrotreating Catalyis, Science and Technology*; Eds. Anderson, J. R., Boudart, M., Springer-Verlag: New York, 1996; Vol. 11. (b) Prins, R.; de Beer, V. H. J.; Somorjai, G. A. "Structure and function of the catalyst and the promoter in cobalt-molybdenum hydrodesulfurization catalysts," *Catal. Rev.-Sci. Eng.* **1989**, *31*, 1. (c) Startsev, A. N. "The mechanism of HDS catalysis," *Catal. Rev.-Sci. Eng.* **1995**, *37*, 353.

51. (a) Wisser, O.; Landa, S. *Sulfide Catalysts. Their Properties and Applications*, Pergamon Press: Oxford, 1973. (b) Delmon, B. "Recent approaches to the anatomy and physiology of cobalt molybdenum hydrodesulfurization catalysts," in *Chem. Uses Molybdenum*, Proc. Int. Conf., 3rd, Barry, H. F.; Mitchell, P. C. H. Eds. (Climax Molybdenum Co., Ann Arbor, 1979), 73. (c) Massoth, F. E.. "Characterization of molybdena catalysts," *Adv. Catal.* **1978**, *27*, 265. (d) Schuit, G. C. A.; Gates, B. C. "Chemistry and engineering of catalytic hydrodesulfurization," *AIChE J.* **1973**, *19*, 417. (e) Grange, P. "Catalytic hydrodesulfurization," *Catal. Rev. - Sci. Eng.* **1980**, *21*, 135. (f) Knoezinger, H. "Genesis and nature of molybdenum-based hydrodesulfurization catalysts," in *Catalysis. Theory to Practice*, Proc. - Int. Congr. Catal., 9th (1988), *5*, 20. (g) Voorhoeve, R. J. H.; Stuiver, J. C. M. "Kinetics of hydrogenation on supported and bulk nickel-tungsten sulfide catalysts," *J. Catal.* **1971**, *23*, 228. (h) Topsøe, N. Y.; Topsøe, H. "Characterization of the structures and active sites in sulfided cobalt-molybdenum/alumina and nickel-molybdenum/alumina catalysts by nitric oxide chemisorption." *J. Catal.* **1983**, *84*, 386. (i) Delmon, B.; Hagenbach, G.; Courty, Ph. "Catalytic activity of cobalt and molybdenum sulfides in the hydrogenolysis of thiophene, hydrogenation of cyclohexene, and isomerization of cyclohexane," *J. Catal.* **1971**, *23*, 29. (j) Hagenbach, G.; Courty, Ph.; Delmon, B. "Physicochemical investigations and catalytic activity measurements on crystallized molybdenum sulfide-cobalt sulfide mixed catalysts," *J. Catal.* **1973**, *31*, 26. (k) Wentrcek, P. R.; Wise, H. "Defect control of hydrogenation activity of molybdenum sulfide catalyst," *J. Catal.* **1976**, *45*, 349. (l) Wentrcek, P. R.; Wise, H. "Hydrodesulfurization activity and defect structure of a cobalt-molybdenum sulfide catalyst," *J. Catal.* **1978**, *51*, 80. (m) Topsøe, H.; Clausen, B. S. "Active sites and support effects in hydrodesulfurization catalysts," *Appl. Catal.* **1986**, *25*, 273. (n) Kemp, R. A.; Ryan, R. C.; Smegal, J. A. "Stacking of molybdenum disulfide layers in hydrotreating catalysts," in ref 51f, *1*, 128.

52. Co, Ni, and Co-Ni promoted MoS_2 on alumina catalysts have been generated ultrasonically and showed a superior hydrodesulfurization activity which presumably arises from the higher dispersion of the MoS_2 on the support and the consequent higher concentration of the catalytically active edge sites. Dhas, N. A.; Ekhtiarzadeh, A.; Suslick, K. S. "Sonochemical preparation of supported hydrodesulfurization catalysts," *J. Am. Chem. Soc.* **2001**, *123*, 8310.

53. Nanostructured & Amorphous Materials, Inc., Cat. No. 3910ZQ.

54. Eliseev, A. A.; Uspenskaya, S. I.; Fedorov, A. A. "About the crystal structure of neodymium disulfide," *Zh. Neorg. Khim.* **1971**, *16*, 1485.

55. Yanagida, S.; Wada, Y.; Hasegawa, Y. "Nano-sized rare-earth oxides or sulfides and their manufacture by photochemical reaction," PCT Int. Appl. 2001, WO 2001-JP4833.
56. Hibble, S. J.; Walton, R. I.; Hannon, A. C.; Bushnell-Wye, G. "The structure of amorphous CrS_3 containing $[Cr_2^{III}((S^I)_2)_3]_x$ chains: an X-ray diffraction modeling study," *J. Solid State Chem.* **1999**, *145*, 573.
57. Lindsley, D. H.; Davis, B. T. C.; MacGregor, I. D. "Ferrosilite ($FeSiO_3$): synthesis at high pressures and temperatures," *Science* **1964**, *144*, 73.
58. Di Paola, A.; Palmisano, L.; Derrigo, M.; Augugliaro, V. "Preparation and characterization of tungsten chalcogenide photocatalysts," *J. Phys. Chem. B* **1997**, *101*, 876.
59. (a) Sriram, M. A.; Kumta, P. N. "The thio-sol-gel synthesis of titanium disulfide and niobium disulfide," *J. Mater. Chem.* **1998**, *8*, 2441. (b) Clapper, T. W. "Titanium disulfide," U.S. 1981, US 80-115993.
60. See for example, (a) Patzke, G. R.; Krumeich, F.; Nesper, R. "Oxidic nanotubes and nanorods - anisotropic modules for a future nanotechnology," *Angew. Chem. . Int. Ed. Engl.* **2002**, *41*, 2446 and references therein. (b) Hakuta, Y.; Ashiri, M.; Arai, K. "Processing nanoscale inorganic materials in supercritical fluids," *J. Soc. Inorg. Mater. Japan* **2001**, *295*, 484. (c) Yoshimura, M.; Somiya, S. "Hydrothermal synthesis of crystallized nano-particles of rare earth-doped zirconia and hafnia," *Mater. Chem. Phys.* **1999**, *61*, 1. (d) Fulton, J. L.; Hoffmann, M. M. "Hydrothermal preparation of rare earth oxide fluoride nanoparticles and nanofibers as aq. phase catalyst supports and corrosion-resistant coatings," PCT Int. Appl. 2001, WO 2000-US24589.
61. Niederberger, M.; Muhr, H.-J.; Krumeich, F.; Bieri, F.; Guenther, D.; Nesper, R. "Low-cost synthesis of vanadium oxide nanotubes via two novel non-alkoxide routes," *Chem. Mater.* **2000**, *12*, 1995.
62. Lu, Q.; Hu, J.g; Tang, K.; Qian, Y.; Liu, X.; Zhou, G. "A simple method for the preparation of nanocrystalline transition metal sulfides," *J. Solid State Chem.* **1999**, *146*, 484.
63. Lu, Q.; Hu, J.; Tang, K.; Qian, Y.; Zhou, G.; Liu, X. "Synthesis of nanocrystalline $CuMS_2$ (M = In or Ga) through a solvothermal process," *Inorg. Chem.* **2000**, *39*, 1606.
64. Li, B.; Xie, Y.; Huang, J. X.; Qian, Y. T. "Synthesis by a solvothermal route and characterization of $CuInSe_2$ nanowhiskers and nanoparticles," *Adv. Mater.* **1999**, *11*, 1456.
65. A ternary transition-metal sulfide has been prepared in an ultrafine power form (100 nm) via solvothermal method. Hu, J.; Lu, Q.; Tang, K.; Qian, Y.; Zhou, G.; Liu, X. "A solvothermal reaction route for the synthesis of $CuFeS_2$ ultrafine powder," *J. Mater. Res.* **1999**, *14*, 3870.
oo. See for example, (a) Suslick, K. S.; Price, G. J. "Applications of ultrasound to materials chemistry," *"Ann. Rev. Mater. Sci.* **1999**, *29*, 295. (b) Jeevanandam, P.; Koltypin, Yu.; Gofer, Y.; Diamant, Y.; Gedanken, A. "Sonochemical synthesis of nanocrystallites of ruthenium sulfide, $RuS_{1.7}$," *J. Mater. Chem.* **2000**, *10*, 2769. (c) Zhu, J.; Liu, S.; Palchik, O.; Koltypin, Y.; Gedanken, A. "A novel sonochemical method for the preparation of nanophasic sulfides: synthesis of HgS and PbS nanoparticles," *J. Solid State Chem.* **2000**, *153*, 342. (d) Avivi, S.; Palchik, O.; Palchik, V.; Slifkin, M. A.; Weiss, A. M.; Gedanken, A. "Sonochemical synthesis of nanophase indium sulfide," *Chem. Mater.* **2001**, *13*, 2195. (e) Nikitenko, S. I.; Koltypin, Y.; Mastai, Y.; Koltypin, M.; Gedanken, A. "Sonochemical synthesis of tungsten sulfide nanorods," *J. Mater. Chem.* **2002**, *12*, 1450.
67. *Teaching general chemistry – A materials science companion*, Ellis, A. B.; Geselbracht, M. J., Johnson, B. J.; Lisensky, G. C.; Robinson, W. R.; Am. Chem. Soc.: Washington D. C., 1993.

68. "Report on the National Science Foundation Undergraduate Curriculum Development Workshop in Materials," October 11-13, 1989. Pub. April 1990.

Nanocrystal-to-Nanocrystal Metathetical Conversion of a Rare-Earth Oxide into a Rare-Earth Polysulfide at Intermediate Temperatures

Li-Ming Wu,[†] Renu Sharma,[‡] Dong-Kyun Seo*[,†]

[†]*Department of Chemistry and Biochemistry, Arizona State University, Tempe, AZ 85287-1604*

[‡]*Center for Solid State Science, Arizona State University, Tempe, AZ 85287-1704*

RECEIVED DATE (will be automatically inserted after manuscript is accepted)

Metathetical reaction of hydrogen sulfide with transition-metal compounds is a common way for the syntheses of nanosized transition-metal sulfides:

$$M_xO_y + yH_2S \rightarrow M_xS_y + yH_2O$$

One well-known example is the preparation of inorganic fullerene-like and nanotubular structures of WS_2 and MoS_2 from their corresponding oxides, WO_3 and MoO_3, in a reducing environment at elevated temperatures.[1 - 3] The substoichiometric oxides that are formed by the reduction at the beginning of the synthesis are volatile and sublime to react with H_2S gas and the nanostructured sulfides deposit at the cold end of the reaction vessel. Low-temperature synthetic methods also have been reported based on solvent-mediated sulfidation of transition-metal halides, carbonyls or alkoxides by H_2S, e.g. sonochemical reactions,[4] sol-gel reactions,[5] and inverse micelle syntheses.[6, 7] The low-temperature reaction products are often amorphous, and need to be annealed at higher temperatures for better crystallinity.[4, 5]

Recently we have found that boron sulfides, which have been relatively unfamiliar as sulfidizing agents, could be a versatile source of sulfur in oxidative sulfidation of metals as well as in metathetical sulfidation of various metal oxides under an intermediate-temperature condition.[8] Known boron sulfides, B_2S_3 and BS_2, are normally obtained as amorphous phases, and they are quite corrosive to silica reaction container typically above 600 °C.[9, 10] However, the volatile nature of these sulfides permits them to react with metals and oxides effectively via solid-gas reactions even in a lower temperature range (300 – 600 °C). In this communication, we report a simple "one-step" nanocrystal-to-nanocrystal synthesis of NdS_2 by sulfidizing Nd_2O_3 with the boron sulfides as a sulfidizing agent.

0.337 g (1 mmol) of Nd_2O_3 powder (99.9 %, 49 – 64 nm, Nanostructured & Amorphous Materials Inc.) was first loaded in a fused silica tube with an excess amount of boron (99.99 %, 325 mesh, Alfa Aesar) and sulfur powder (99.999 %, Alfa Aesar) of 2:3 ratio. After the tube was evacuated and flame-sealed, the reaction mixture was gradually heated to 450 °C, kept at the temperature for one day, and radiatively cooled down to room temperature. The pale violet color of the original powder turned into grayish yellow after the reaction. Figure 1 compares the powder X-ray diffraction (XRD) patterns of the original Nd_2O_3 particles and our reaction product NdS_2, and indicates that the Nd_2O_3 was completely converted into an X-ray pure NdS_2 product. It is noted that the sulfide product is the most sulfur-rich phase in the Nd–S binary system, and not the corresponding stoichiometric compound, Nd_2S_3. NdS_2 exhibits square layers of

* To whom correspondence should be addressed. E-mail: DSeo@asu.edu

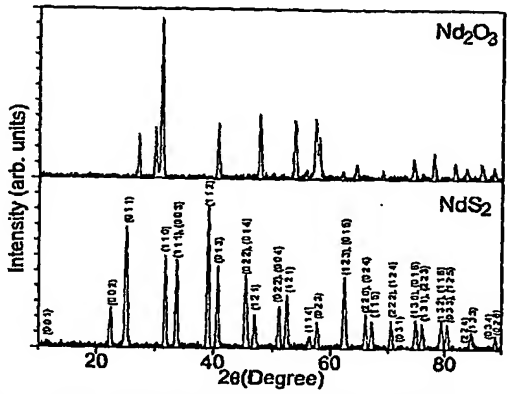

Figure 1. The powder XRD patterns of the Nd_2O_3 and NdS_2 nanoparticles.

covalently-bonded sulfur atoms in its bulk tetragonal layered structure, and the polysulfide unit is likely due to the intermediate-temperature reaction condition in addition to the incomplete *in situ* reaction of boron with sulfur. Intermediate temperature conditions are generally considered as a necessary condition for polysulfide preparations.[11] Overall reaction occurs as follows:

$$Nd_2O_3 + 2B + 4S \rightarrow 2NdS_2 + B_2O_3$$

Unreacted sulfur, boron sulfides and the byproduct B_2O_3 were washed away from the product by using CS_2 and deionized water, and the filtered powder sample was found to be boron-free based on our atomic absorption spectrometric analysis within the detection limit (5 ppm) of the instrument (Varian SpectrAA-400 Flame). Samples for high resolution transmission electron microscopy (HRTEM) studies were prepared by dispersing a few drops of the suspensions of this powder and Nd_2O_3 respectively in deionized water on holey carbon grids. A JEOL 4000 EX transmission electron microscope (TEM), operated at 400 kV (1.7 Å point resolution) was used to obtain HRTEM images. The crystals were oriented along various zone axes using a double-tilt stage, and HRTEM images were recorded on photographic films.

Comparison of the HRTEM images of both the Nd_2O_3 starting material and our NdS_2 product revealed that the original size and shape of the Nd_2O_3 were well maintained after the sulfidation process as shown in the representative images (Figures 2a and 3a). The disk-like shape of both Nd_2O_3 and NdS_2 nanoparticles could be from the layer-like nature of the structures of the two compounds (Figure 4).[12, 13] The Nd_2O_3 structure is formed by $\{(Nd_2O_2)^{2+}\}$ and $\{O^{2-}\}$ layers alternating along *c*-axis of its hexagonal unit cell, while the NdS_2 structure is made of

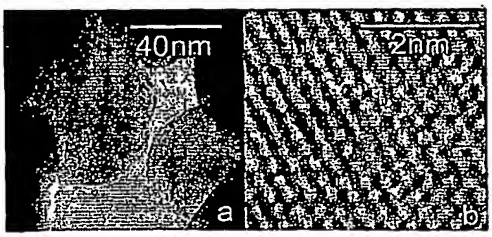

Figure 2. HRTEM micrographs of the Nd_2O_3 nanodisks (starting material). (b) is a zoomed image around the center of (a).

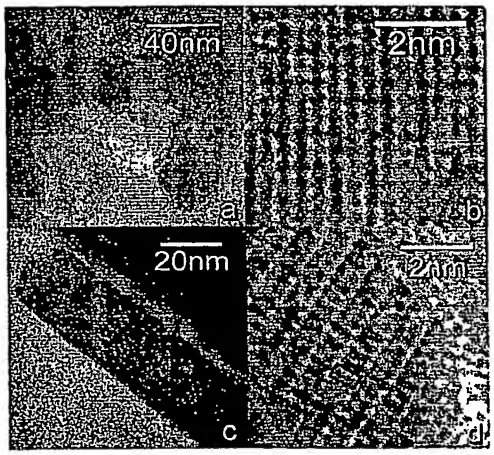

Figure 3. HRTEM micrographs of NdS_2 nanoparticles (product). (b) is a representative zoomed image from the top of the disks in (a). (c) Side-view of an NdS_2 nanodisk. (d) Representative zoomed image of the side of NdS_2 nanodisk around a corner.

$\{(Nd_2S_2)^{2+}\}$ and $\{S_2^{2-}\}$ layers that also alternate along *c*-axis of its tetragonal unit cell.[14] Indeed, a closer look perpendicular to the Nd_2O_3 nanodisks, i.e. along <001> direction (Figure 2b), reveals a hexagonal symmetry that reflects the atomic arrangement in *ab*-plane of the Nd_2O_3 structure. The measured repeat distances (3.8 Å along the two in-plane axes), are in good agreement with the reported value of the bulk structure (a = 3.83 Å). Meanwhile, the corresponding HRTEM images of the NdS_2 nanodisks oriented along <001> direction (Figure 3b), reveals that the atoms are arranged in a square lattice with a repeat distance of 4.0 Å along the two perpendicular directions with a very good crystallinity. The measured lattice spacing matchs well with the a-spacing (4.022 Å) of the unit cell of the bulk NdS_2. Figure 3c is a side-view of an NdS_2 nanodisk with thickness of ca. 30 nm. This nanocrystal was found to be oriented along <010> direction, and the high magnification image is shown in Figure 3d. The measured repeat distances of the two-dimensional rectangular unit cell in Figure 3d, 4.0 Å and 8.0 Å, are consistent with a (or b) and c unit cell parameters of the bulk NdS_2 structure, (4.022 and 8.031 Å, respectively). It is not clear yet if the same disk-like shapes of the starting material and the final product are due to the similar type of the layered structures of Nd_2O_3 and NdS_2. We are currently investigating the effect of structural relationships between oxides and sulfides on the shape and crystallinity of the sulfidized nanoparticles by employing nanoparticles of other rare-earth and transition-metal oxides as starting materials.

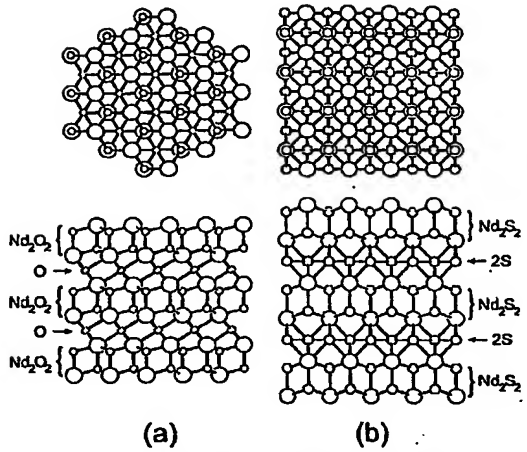

Figure 4. Top and side views of (a) Nd_2O_3 and (b) NdS_2. Large and small circles represent Nd and O (or S) atoms. Sulfur-sulfur bonds are shown in thin line in (b). Nd atoms are drawn larger to emphasize the higher electron density.

In conclusion, by using boron sulfides as a source of sulfur, we have successfully converted nanocrystals of Nd_2O_3 into nanocrystals of a rare-earth metal polysulfide NdS_2 without any noticeable fusion of the particles. The intermediate-temperature reaction condition is important for the polysulfide formation and the reaction temperature was high enough to afford a good crystallinity without a further thermal treatment. While binary and ternary transition metal oxides are easily available in various nano-sized forms, the corresponding nanostructured sulfides are relatively rare despite their technological importance. We expect that this simple one-step sulfidation process could be an alternative synthetic route for various nanosized metal sulfide materials that are not easy to be prepared by other means.

References
(1) Feldman, Y.; Wasserman, E.; Srolovitz, D. J.; Tenne, R. *Science* 1995, 267, 222.
(2) Rothschild, A.; Sloan, J.; Tenne, R. *J. Am. Chem. Soc.* 2000, 122, 5169.
(3) Whitby, R. L. D.; Hsu, W. K.; Kroto, H. W.; Walton, D. R. M. *Phys. Chem. Chem. Phys.* 2002, 4, 3938.
(4) Mdleleni, M. M.; Hyeon, T.; Suslick, K. S. *J. Am. Chem. Soc.* 1998, 120, 6189.
(5) Sriram, M. A.; Kumta, P. N. *J. Am. Ceram. Soc.* 1994, 77, 1381.
(6) Wilcoxon, J. P.; Samara, G. A. *Phys. Rev. B* 1995, 51, 7299.
(7) Wilcoxon, J. P.; Newcomer, P. P.; Samara, G. A. *Solid State Commun.* 1996, 98, 581.
(8) Wu, L.-M.; Seo, D.-K. manuscripts in preparation.
(9) Gerhartz, W.; Yamamoto, Y. S.; Campbell, F. T.; Pfefferkorn, R.; Rounsaville, J. F. Eds. *Ullmann's Encyclopedia of Industrial Chemistry*, Vol A4, VCH Publishers: Weinheim, 1985, p315.
(10) Conrad, O.; Jansen, C.; Krebs, B. *Angew. Chem, Intern. Ed.* 1998, 37, 3209 and references therein.
(11) Vasilyeva, I. G. "Polysulfides" in *Handbook on the Physics and Chemistry of Rare Earths* Vol. 32 Gschneidner, Jr., K. A.; Eyring, L.; Lander, G. H. Eds. Elsvier; Amsterdam: 2001, and references therein.
(12) Boucherle, J. X.; Schweizer, J. *Acta Cryst. B* 1975, 31, 2745.
(13) Eliseev, A. A.; Uspenskaya, S. I.; Fedorov, A. A. *Zh. Neorg. Khim.* 1971, 16, 1485.
(14) Two polymorphs with slight distortions from the tetragonal structure have been reported for NdS_2 from single-crystal X-ray crystallography studies. Our powder XRD and HRTEM studies did not distinguish the small distortions.

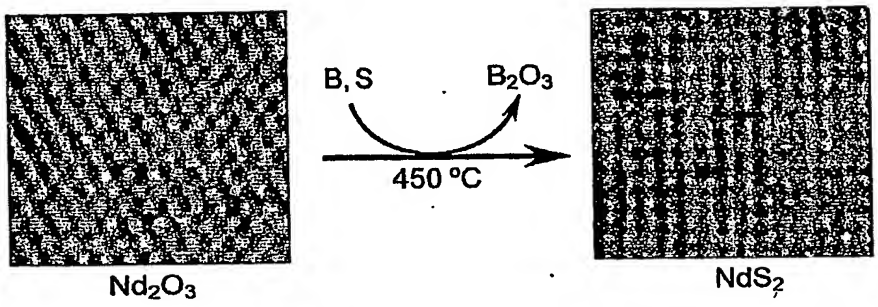

By employing boron sulfides that were prepared *in situ* as a source of sulfur, Nd_2O_3 nanoparticles were successfully converted into NdS_2 under an intermediate temperature condition, while the original sizes and crystallinity of the particles were preserved. This work demonstrates that this simple one-step sulfidation process could be an alternative synthetic route for various nanosized metal sulfide materials that are not easily available by other means.

A Simple Route to the Neat High-Yield Preparation of Nanostructured Tungsten Disulfide

Li-Ming Wu, Dong-Kyun Seo*
Department of Chemistry and Biochemistry, Arizona State University, Tempe, AZ, 85287-1604

Layered material tungsten sulfide (2H-WS_2) is commonly used as solid lubricants [1,2] and as additives in liquid lubricants. [3,4] Minimum tangential resistance is commonly associated with shearing of the weak inter-layer sulfur atoms bond (typically van der Waals (vdW)) in these materials.[5,6] In addition, WS_2 is also a very important catalyst which has been used for the removal of sulfur and nitrogen from petroleum feedstocks for over 50 years.[7,8] WS_2 nanoparticles were expected more excellent lubricated and catalysis properties due to special morphology, smaller size and larger surface areas.[9,10,11,12]

The first WS_2 nanotubes and fullerene-like nanoparticles were observed by hydrosulfurization of a very thin film of tungsten metal (several hundreds Å). [13] Recently, synthesis method of WS_2 nanoparticles has been focused on high temperature methods, which occur above 800°C with tungsten oxides. These methods involve such techniques as growth from the gas phase in which tungsten oxides in the vapor phase are reacted with H_2S in a carrier gas producing WS_2 nanoparticles. [14] With this methods, WS_2 fullerene-like nanoparticles[15,16], nanotubes[17-20], foils[17], ribbons[18] and ropes[18] can be got in the temperature range from 800°C to 1200°C based on the reaction as shown in equation (1):

$$WO_{3-x} + H_2S \rightarrow WS_2 + H_2O \quad (1)$$

To convert tungsten oxides to tungsten sulfides nanoparticles pre-synthesized tungsten oxides nanoparticles is required. For example: WS_2 fullerene-like nanoparticles are synthesized starting with WO_3 powder with particles sizes smaller than ca. 150nm. [15,16] In synthesis of WS_2 nanotubes, WO_x nanorods(x=2-3, ~100μm length and 10-100nm diameter) also need to be generated first. [20] So with this method, for orientating the growth to a phase composed in its greatest majority of WS_2 nanoparticles, an asymmetric tungsten oxide precursor, which contains already the "future shape" of a nanoparticles, was needed. [19]

Recently, people found that the $W(CO)_6$ also can be used as a starting materials to synthesize WS_2 nanoparticles. For example the morphology of the WS_2 nanoparticles can be got from sulfidizing $W(CO)_6$ with H_2S solution in argon in a 0.915 to 2.45 GHZ microwave plasma in a temperature range from 160°C to 580°C. This method produces to relatively small and uniform patticles. [21] The other report is WS_2 nanoparticles can be obtained from $W(CO)_6$ by dissolving the $W(CO)_6$ and S in diphenylmethane, then heating and sonicating the mixture in an argon flow for 3h.

Up to now, synthesis of WS_2 nanoparticles needs complicated devices or special nanoparticles as starting materials. So as said by R.R.Chianelli's "The study of these materials has been hindered by the inability to synthesize them in large quantities. This situation is similar to early days of research in fullerens that progress slowly until improved synthetic method led to large quantities being available."[14]

Recently we found the boron sulfide can act as very strong sulfidizing agent even at intermediate temperature (<600°C). To date, boron sulfides (B_2S_3 and BS_2) have not been know well as sulfidizing agents, and their use has been reported only in organic or organometallic reactions, yet sporadically. [21-23] There exist only two boron sulfides, namely, B_2S_3 and BS_2, in the sulfur-rich end, and both of the air-sensitive compounds are normally obtained in amorphous phase. [24] B_2S_3 does not have a well-defined melting point, but begins to sublime at about 300 °C. [25] BS_2, the only boron sulfide with a higher content of sulfur, melts congruently at 417°C under atmospheric pressure. [26] However, our experiences show that a significant amount of BS_2 evaporates even at 300 °C under vacuum.

High temperature (around 1000°C) is required for hydrosulfurize tungsten film (several hundreds Å) with H_2S. [13] Using boron sulfides as sulfurizing agent, we found the reaction can be done completely at 500°C even with 0.2mm diameter W wires. In this paper, we present a novel efficient method for synthesis WS_2 nanoparticles directly using 0.2mm W wires as the starting materials to react with boron sulfide at 500°C in situ. Low temperature is important and favorite for synthesis of nanosize particles. For example: for converting the WO_3 nanoparticles to WS_2, the reaction need to be run around 900°C. In such a high temperature, in order to avoid agglomeration and fusion of the heated nanoparticles, the powder need to be very carefully dispersed on the entire floor of the reactor boat.[16] This limit is a disadvantage for synthesis WS_2 nanoparticles in large quantities.

Tungsten metal directly reacts with sulfur only at high temperature. Using boron sulfides as sulfidizing agent can make the reaction processing at lower temperature. In our system, the boron powders reacted with sulfur formed boron sulfide first. Then the tungsten wires were sulfidized by boron sulfides at low temperature, as following:

$$B + S \rightarrow BS_x \qquad (2)$$

$$W + BS_x \rightarrow WS_2 + B \qquad (3)$$

The boron reduced by tungsten can continue to react with sulfur and further form boron sulfide under excess sulfur existing. It seems that the boron sulfides act as a catalysis, which catalyze tungsten silfidization at low temperature.

After reaction, the product maintained the original shape of the tungsten wires, but with a roughly doubled thickness. The surface exhibited severe cracks along the wire axis, and the product was easy to grind into a fine powder. We clean and sonicate the samples with water for 30mins, and get hightly fine and pure powders. Figura.1 present the X-ray power diffraction pattern (XPD) of this fine WS_2 powders. From the XPD, it can be assigned that the products are 2H-WS_2. As shown in Fig.1, the Bragg peaks are very broad, indicating small sizes of the powder particles. One intriguing feature is that the (00*l*) peaks are shifted toward lower angles, indicating the expansion of the lattice along the *c*-axis, in comparison with the bulk 2H-phase (vertical lines).[27] The shift of $\Delta c = 0.14$ Å was calculated using synthetic silicon as an internal standard for the powder diffraction studies. The same observation was made from our molybdenum sulfidation reactions. A similar shift has been reported for the fullerene-like and nanotubular structures of WS_2 and MoS_2 ($\Delta c = 0.16$ and 0.25 Å, respectively), [28, 29] and attributed to a strain relief in the folded structures by expanding the spacing between adjacent layers. This has been known for carbon fullerenes and nanotubes as well.[30-32]

Figure 2 shows the scanning electron microscope (SEM) images of the shape and the surfaces of tungsten wires after sulfization. From the images we can see the samples already crack to small particles along the wire axis (Fig.2a), and the surfaces of samples form by stacking with some thin layers in thicknesses range from 100nm to several hundreds nm (Fig. 2b). And even every layer also forms by congregating with a lot of smaller particles with size distribution from several nanometers to tens nm (Fig.2c). Although the WS_2 samples still keep the wire shape, but actually they just simply accumulate by a lot of small WS_2 nanoparticles. So they are crisp and easy to be ground to small powders. After sonicated in acetone for 30mins, the wire-shape samples almost were crushed to fine WS_2 powders. The SEM images of those samples after sonicated were given in Figure 3. The images show that the WS_2 nanoparticles are irregular small pieces and very thin. The thicknesses of those nanoparticles just are around 10 nm. The widths of those particles change from several nm to around 100nm.

Two HRTEM pictures of WS_2 nanoparticles were presented in Figure 4. As seen from the image, there are lot boundaries areas exist in our samples because the size of particle is small and the shapes are random. Fig. 4b shows the TEM image of boundary area. There are some fringes whose spaces are around 6.3Å, which can be index to the WS_2 layer distances in the bulk structure (6.16Å[27]). But the fringes aren't parallel each other like which existing in the crystal. There are distortions, coalitions, intercrosses and even can be curve at the boundary areas. It causes the WS_2 layer distances increasing and changing a little bit larger than the layer distance 6.16Å. And it also causes the space between differences layers isn't fixed to a constant but change in a range. So in the XPD image, the Bragg peaks become broader and have a little bit shift to low angle area. In catalysis, the edge plane is highly reactive. And in generally, a poorly crystalline and highly disordered state can lead to good catalytic properties. So with a lot of disorder boundary areas in our samples may possess good catalytic properties.

In conclusion, using boron sulfide as sulfurization agent, WS_2 nanoparticles can be synthesized starting with 0.2mm diameter tungsten wires as a starting materials. This is a very simple and efficient way for bulk synthesis of WS_2 Nanoparticles. The SEM and TEM tests show that the shapes of WS_2 nanoparticles what we get are irregular small pieces. They are very thin. The thicknesses of those nanoparticles are around 10 nm. The width of those particles can change from several nm to about 100nm. They also show our samples have a lot boundary area exist which can explain the result of the broad Bragg peaks peak and lower angle shift in XPD test. And with a lot of disorder boundary, the samples are excepted have good catalytic properties. It is noted that we obtained very similar results for the synthesis of molebdenium disulide.

Experimental:

WS_2 nanoparticles were prepared by direct sulfidize tungsten wire (0.2mm in diameter, ~5cm long) in situ with boron sulfides. The tungsten (wire, 99.95%), boron (powder, -325mesh, 99.99%) and sulfur (Pieces, 99.999%) were obtained from Aldrich. All those materials were used without further purification. We put two small size silicon crucibles in a big silicon tube. The upper crucible contains tungsten wire (0.5515g, 3mmol) and the lower crucible carries boron (0.0324g, 3mmol) and sulfur (0.3847, 12mmol). Separating tungsten and boron with two small silicon tubes can avoid the remained boron contaminating products WS_2. After the tube was evacuated and sealed, the reaction

mixture was gradually heated to 500°C, kept at the temperature for 3 days, and radiatively cooled down to room temperature. The sample was washed with a lot of distilled water to get ride of B_2S_3.

For testing the remainder concentration of boron with atomic adsoption spectrum, we dissolve 50mg WS_2 in 5ml Aqua Regla. No boron signals were found under atomic adsoption spectrum testing with 5ppm test limit. It shows that the remainder concentration of boron is smaller than 0.05% (weight percent).

After first step reaction and cleaning, the samples keep the original wire shape. But the samples are very crisp. Sonicating the samples for 30mins, the samples completely convert to fine WS_2 nanoparticles.

The resulting products were characterized by X-ray powder diffraction (XRD) using a Siemens power diffractometer High-resolution scanning electron microscopy (HRSEM) measurements were performed using a Hitachi S-4700-II. High-resolution transmission electron microscopy (HRTEM) analysis was carried out using a JEOL JEM 4000EX. And the elements analysis for remained boron test with atomic adsoption spectrum technology using Varian SpectrAA-400 Flame.

References:

[1] F.P.Bowden, D.Tabor, *The Friction and Lubrication of Solids, Part II*, Oxford Univ. Press, London **1964**.

[2] B.Bhushan, B.K.Gupta, *Handbook of Tribology*, McGraw-Hill, New York **1991**.

[3] A.L.Black, R.W.Dunster, J.V. Sanders, *Wear* **1969**,13,119.

[4] J.Gansheimerand, R.Holinsky, *Wear* **1972**,19,439.

[5] F.P.Bowden, D.Tabor, *Friction: An Introduction to Tribology, Vol.91*, Anchor, Garden city, New York **1973**.

[6] I.L.Singer, *in Fundamentals of Friction: Macroscopic and Microscopic Processes* (eds I.L.Singer, H.M.Pollock), Kluwer, Dordrecht **1992**.

[7] O.Weiser, S.Landa, *Sulfide Catalysts: Their Properties and Applications*, Pergamon, Oxford **1973**.

[8] M.Daage, R.R.Chianelli, *J.Catal.* **1994**,149,414.

[9] L.Rapoport, V.Leshchinsky, M.Lvovsky, O.Nepomnyashchy, Y.Volovik, R.Tenne, *Wear* **2002**,252,518.

[10] L. Rapoport, M. Lvovsky, I. Lapsker, V. Leshinsky, Y. Volovik, Y. Feldman, A. Zak, R. Tenne, *Adv.Eng.Mater.* **2001**,3,71.

[11] R.R.Chianelli, M.Daage, *Advances in Catalysis Vol.40* , Academic Press, London **1994**.

[12] D.H.Galvan, G.Alonso, R.Rangle, M.Del Valle, E.Adem, S.Fuentes, *J.Catal.* **2000**, 189, 263.

[13] R.Tenne, L.Margulis, M.Genut, G.Hodes, *Nature* **1992**, 360, 444.

[14] R.Rchianelli, G.Berhault, P.Santiago, D.Mendoza, A.Espinosa, J.A.Ascencio, M.J.Yacaman, *Mater. Tech.* **2000**, 15, 54.

[15] Y.Feldman, V.Lyakhovitskaya, R.Tenne, *J.Am.Chem.Soc.* **1998**,120,4176.

[16] Y.Feldman, G.L.Frey, M.Homyonfer, V.Lyakhovitskaya, L.Margulis, H.Cohen, G.Hodes, J.L.Hutchison, R.Tenne, *J.Am.Chem.Soc.* **1996**,118,5362.

[17] R.Rosentsveig, A.Margolin, Y.Feldman, R. Popovitz-Biro, R.Tenne, *Chem. Mater.* **2002**,14,471.
[18] M.Remakar, Z.Skraba, M.Regula, C.Ballif, R.Sanjines, F.Levy, *Adv.Mater.* **1998**,10,246.
[19] A.Rothschild, J.Sloan, R.Tenne, *J.Am.Chem.Soc.* **2000**,122,5169.
[20] Y.Q.Zhu, W.K.Hsu, N.Grobert, B.H.Chang, M.Terrones, H.Terrones, H.W.Kroto, D.R.M.Walton, *Chem.Mater.* **2000**, 12, 1190.
[21] R.R.Schumaker, E.M.Engler, *J. Am. Chem. Soc.* **1977**, 99, 5521.
[22] K.P.Callahan, P.J.Durand, *Inorg. Chem.* **1980**, 19, 3211.
[23] A.A.Eagle, E.R.T.Tiekink, G.N.George, C.G.Young, *Inorg.Chem.*, **2001**, 40, 4563.
[24] N.N.Greenwood, A.Earnshaw, *Chemistry of the elements*, Pergamon Press: Oxford **1984**.
[25] W.Gerhartz, Y.S.Yamamoto, F.T.Campbell, R.Pfefferkorn, J.F.Rounsaville, *Ullmann's Encyclopedia of industrial chemistry, Vol A4*, VCH,Weinheim **1985**
[26] Z.S.Medvedeva, V.A.Boryakova, Y.K.Grinberg, E.G.Zhukov, *Zh. Neorg. Khim.* **1968**, 13, 1440.
[27] W. J.Schutte, J. L.de Boer, F.Jellinek, *J. Solid State Chem.* **1987**, *70*, 207.
[28] A.Zak, Y.Feldman, V.Lyakhovitskaya, G.Leitus, R.Popovitz-Biro, E.Wachtel, H.Cohen, S.Reich, R.Tenne, *J. Am. Chem. Soc.* **2002**, *124*, 4747.
[29] Y.Feldman, E.Wasserman, D.J.Srolovitz, R.Tenne, *Science* **1995**, *267*, 222.
[30] Y.Saito, T.Yoshikawa, S.Bandow, M.Tomita, *Phys. Rev. B* **1993**, *48*, 1907.
[31] Y.Yosida, *Appl. Phys. Lett.* **1994**, *64*, 3048.
[32] M.Li, J.M.Cowley, *Ultramicroscopy* **1994**, *53*, 333.

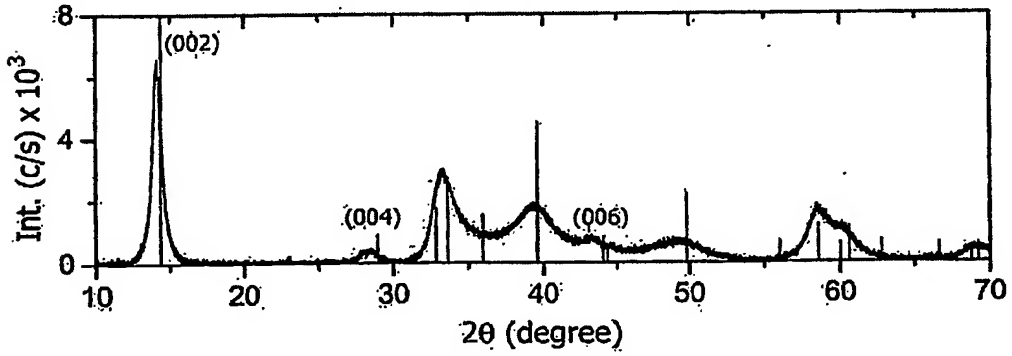

Fig.1. XRD powder pattern of the reaction product from the sulfidation of tungsten wire by boron sulfides. The vertical lines are the Bragg peaks of NBS 2H-WS_2. Note the shift of (00*l*) peaks. The (008) peak is very weak and cannot be seen due to the overlap with a peak of high intensity.

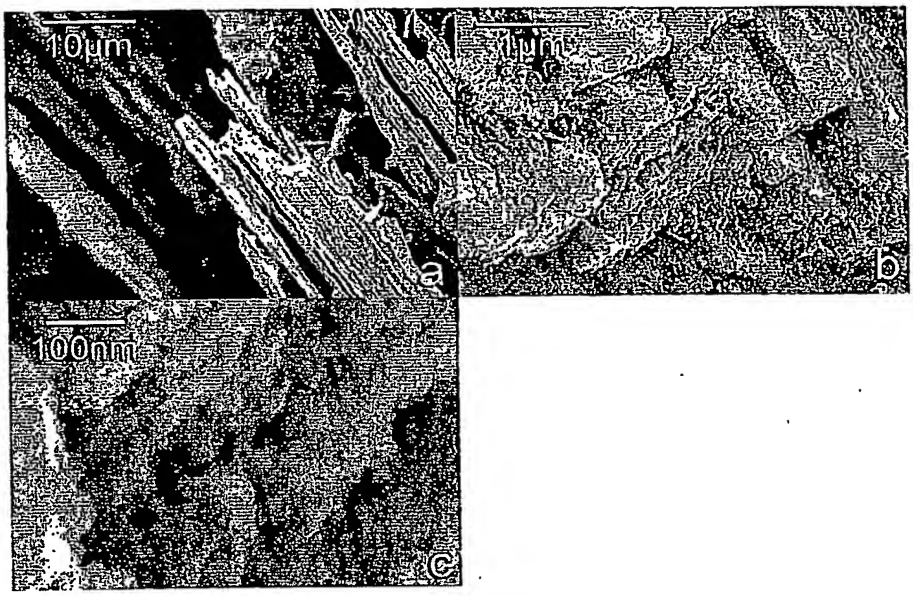

Fig. 2. Low-magnification and higher magnification SEM images of tungsten sulfide. (a) The tungsten sulfide keeping wire shape but cracks along the wire axis. (b) Layers stack on the surface. (c) The layer from by small WS_2 nanoparticles.

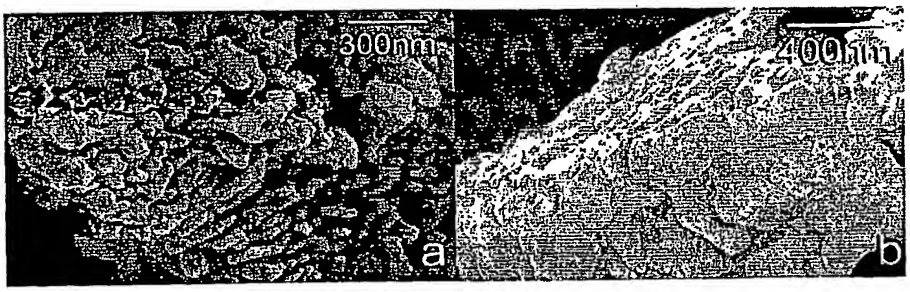

Fig.3. The SEM images of WS_2 after cleaned and sonicated.

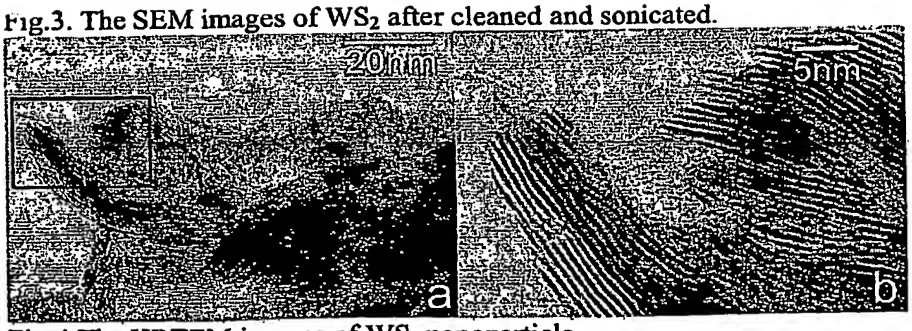

Fig.4.The HRTEM images of WS_2 nanoparticle.

This Page is Inserted by IFW Indexing and Scanning Operations and is not part of the Official Record

BEST AVAILABLE IMAGES

Defective images within this document are accurate representations of the original documents submitted by the applicant.

Defects in the images include but are not limited to the items checked:

- ☐ BLACK BORDERS
- ☐ IMAGE CUT OFF AT TOP, BOTTOM OR SIDES
- ☐ FADED TEXT OR DRAWING
- ☑ BLURRED OR ILLEGIBLE TEXT OR DRAWING
- ☐ SKEWED/SLANTED IMAGES
- ☑ COLOR OR BLACK AND WHITE PHOTOGRAPHS
- ☐ GRAY SCALE DOCUMENTS
- ☐ LINES OR MARKS ON ORIGINAL DOCUMENT
- ☐ REFERENCE(S) OR EXHIBIT(S) SUBMITTED ARE POOR QUALITY
- ☐ OTHER: _____

IMAGES ARE BEST AVAILABLE COPY.
As rescanning these documents will not correct the image problems checked, please do not report these problems to the IFW Image Problem Mailbox.